TAMPEREEN TEKNILLINEN YLIOPISTO
TAMPERE UNIVERSITY OF TECHNOLOGY

TUOMAS MANSIKKALA

ENHANCING THE STRUCTURAL MATURATION AND ATTACHMENT OF HUMAN INDUCED PLURIPOTENT STEM CELL DERIVED CARDIOMYOCTYES ON TEXTILE SURFACES

Master of Science Thesis

Examiner: prof. Minna Kellomäki
Examiner and topic approved by the Faculty Council of the Faculty of Natural Sciences on 06.04.2016

ABSTRACT

TUOMAS MANSIKKALA: Enhancing the Structural Maturation and Attachment of Human Induced Pluripotent Stem Cell Derived Cardiomyocytes on Textile Surfaces
Tampere University of Technology
Master of Science Thesis, 74 pages
February 2017
Master's Degree Programme in Biotechnology
Major: Tissue Engineering
Examiner: Professor Minna Kellomäki

Keywords: cardiomyocyte, coating, human induced pluripotent stem cell, maturation, polyethylene terephthalate, textile

Cardiovascular diseases are one of the leading causes of death in the world. In 2012 ~30% of all deaths were due to cardiovascular diseases. There is a need for new research, drug testing and treatment methods. Tissue engineering and cell culturing can be used to create new models and in future even treatments. Human cardiomyocytes (CMs) have been hard to obtain for research, requiring heart biopsies or human embryonic stem cells. That has been changed by the discovery of human induced pluripotent stem cells (hiPSC). Cells harvested from adults can be induced back to pluripotent stem cells that can be then differentiated to hiPSC derived CMs (hiPSC-CMs). HiPSC maintain the genome of the patient, which allows the study of specific changes and their effects in the genome. One problem with hiPSC-CMs is that they do not have all the functional and morphological properties of adult CMs when cultured on normal *in vitro* conditions. The aim of this study was to determine if using differently coated textiles as culturing surfaces, would create structurally more mature hiPSC-CM.

The hiPSC were differentiated into CMs by END-2 and small molecule method. The produced hiPSC-CM were cultured on textiles coated with either gelatin, collagen, Matrigel or Geltrex. To increase the attachment of gelatin, some of the textiles samples were modified with dopamine or plasma treatment. The controls were grown on gelatin and Geltrex coated cover slips. The analysis was made with immunocytochemistry and fluorescence microscopy. The samples were labelled with antibodies against sarcomere proteins. Live/dead staining was used to determine cell attachment. The shape of hiPSC-CM and its sarcomere organization, orientation and length were analyzed from the immunostaining images using Cytospectre software.

The structural maturation of hiPSC-CMs was evaluated between all coatings and textile structures and they were compared to the hiPSC-CMs grown on coverslips. The cells attached to the textiles, but large portion of the cells passed through the textiles and was left on the bottom of the growth well. The textile grown hiPSC-CMs had more adult like shape and sarcomere structure, but there was no difference in sarcomere lengths. No clear difference between coatings was detected.

Based on the result, the textile structure has a bigger effect on structural maturity than coating material, which only seem to the affect attachment of the cells. This study only established the increase in structural maturity. In the future, it has to be tested if these changes cause any functional improvements.

TIIVISTELMÄ

TUOMAS MANSIKKALA: Pinnoitusmateriaalien vaikutus ihmisen uudelleenohjelmoiduista kantasoluista erilaistettujen sydänlihassolujen kiinnittymiseen ja aikuistumiseen tekstiilipinnalla
Diplomityö, 74 sivua
Helmikuu 2017
Biotekniikan diplomi-insinöörin tutkinto-ohjelma
Pääaine: Kudosteknologia
Tarkastaja: professori Minna Kellomäki

Avainsanat: sydänlihassolu, pinnoite, ihmisen uudelleenohjelmoitu kantasolu, kypsyminen, polyetyleenitereftalaatti, tekstiili

Sydän- ja verisuonitaudit ovat yksi maailman johtavista kuolinsyistä. Vuonna 2012 ~30% kaikista maailman kuolemista aiheutui sydän- ja verisuonitaudeista. Tämän takia on tarvetta uudelle tutkimukselle, lääketestaukselle ja hoitokeinoille. Kudosteknologiaa ja soluviljelyä käyttäen voidaan luoda uusia tutkimus- ja hoitomalleja. Perinteisesti ihmisen sydänlihassolut (CMs) ovat olleet hankalia saada tutkimustarkoitukseen, mutta se muuttui ihmisen uudelleenohjelmoitujen kantasolujen löytymisen (hiPSC) jälkeen. Solut voidaan kerätä aikuiselta ihmiseltä, jonka jälkeen ne uudelleen ohjelmoidaan kantasoluiksi, jotka voidaan sitten erilaistaa sydänsoluiksi. Uudelleen ohjelmoiduista kantasoluista erilaistetut sydänsolut säilyttävät potilaan genomin, mikä mahdollistaa genomin vaikutuksen tutkimisen. Valitettavasti *in vitro*-olosuhteissa uudelleen ohjelmoiduista kantasoluista tuotetut sydänsolut eivät ole olleet toiminnallisilta ja rakenteellisilta ominaisuuksiltaan aikuismaisia. Tämän työn tarkoitus on selvittää, saadaanko aikuismaisuutta lisättyä kasvattamalla soluja pinnoitetuilla tekstiileillä.

Solut erilaistettiin sydänsoluiksi END-2 ja pienmolekyyli metodeilla. Saatuja sydänsoluja kasvatettiin tekstiileillä, jotka oli pinnoitettu joko gelatiinilla, kollageenilla, Geltrexillä tai Matrigeelillä. Osa tekstiileistä käsiteltiin plasmalla tai dopamiinilla gelatiinin kiinnittymisen parantamiseksi. Analysointi tehtiin immunosytokemialla ja fluoresenssimikroskopialla. Immunovärjäystä käytettiin sarkomeeriproteiinien havaitsemiseen. Solujen kiinnittymistä tutkittiin live/dead-värjäyksellä. Solujen muoto ja sarkomeerien rakenne, järjestys ja pituus analysoitiin immunovärjäksistä Cytospectre ohjelmalla.

Kantasoluista tuotettujen sydänsolujen rakenteellinen kypsyminen tutkittiin kaikkien pinnoitusten ja tekstiilien välillä ja niitä verrattiin lasilevyillä kasvatettuihin soluihin. Solut kiinnittyivät tekstiileihin, mutta osa niistä kulkeutui tekstiilin läpi kasvatuskaivon pohjalle. Tekstiileillä kasvatetuilla soluilla oli aikuismaisempi muoto ja sarkomeeri-rakenne, mutta sarkomeerien pituus ei muuttunut. Eri pinnoitteiden välillä ei havaittu selkeitä eroja

Tulosten perusteella tekstiilin rakenteella on suurempi vaikutus solujen aikuistumiseen kuin pinnoitteilla, jotka näyttivät vaikuttavan vain kiinnittymiseen. Tämä tutkimus näytti vain rakenteellisen aikuistumisen paranemisen eikä ottanut kantaa toiminnallisten ominaisuuksien aikuistumiseen.

PREFACE

This Master's Thesis was made for Heart Group, which is one of the regenerative medicine groups in BioMediTech, a joint institute of Tampere University and Tampere University of Technology

First, I would like to thank Katriina Aalto-Setälä, the leader of the Heart Group, for the opportunity to do my thesis in her group. I want to thank my supervisor Mari Pekkanen-Mattila for all the guidance, help and feedback I got during my work. Other special thanks go for Risto-Pekka Pölönen who helped me a lot with Cytospetre and other work methods, Janne Koivisto who helped me with all kinds of problems that came up during the work and Anni Junnila who guided me through the basic methods which I used during this work. I would also like to thank all the other members of Heart Group for their support and the great work atmosphere.

I would like to thank my examiner Minna Kellomäki for giving part of her valuable time to make this thesis possible, and Elina Talvitie for preparing the textile samples for me.

Lastly, I would like to thank my family and friends who kept pushing me forward when I needed it.

Tampere 21.02.2017

Tuomas Mansikkala

TABLE OF CONTENTS

LIST OF FIGURES

LIST OF TABLES

LIST OF SYMBOLS AND ABBREVIATIONS

ATP	adenosine triphosphate
ADP	adenosine diphosphate
BMP	bone morphogenetic protein
bFGF	basic fibroblast growth factor
CM	cardiomyocyte
DAPI	4′,6-Diamidine-2′-phenylindole dihydrochloride
Dkk-1	Dickkopf homolog 1
DMEM	Dulbecco's modified Eagle's medium
EB	embryoid body
ECM	extracellular matrix
EGF	epidermal growth factor
END-2	mouse endothermal-like cell line
FBS	fetal bovine serum
FGF	fibroblast growth factor
GAG	glycosaminoglycan
hiPSC	human induced pluripotent stem cell
hiPSC-CM	human induced pluripotent stem cell-derived cardiomyocyte
hPSC-CM	human pluripotent stem cell-derived cardiomyocyte
iPSC	induced pluripotent stem cell
HA	Hyaluronan
ko-SR	knockout serum replacement
MyBPC	myosin-binding protein C
NEAA	non-essential amino acids
PET	polyethylene terephthalate
PLDLA	poly-(L/D)-lactide
TCPS	tissue culture polystyrene control
TGF-β	transforming growth factor beta
Tm	tropomyosin
Tn	troponin
VEGF	vascular endothelial growth factor

1. INTRODUCTION

Cardiovascular diseases are one of the leading causes of death in the world. In 2012 ~30% of all deaths were due to cardiovascular diseases. (World Health Organization 2015) This creates a need for new research models, drug testing models and treatments. One approach is to use tissue engineering and cell culturing to create the models needed. The problem is the availability of cardiomyocytes (CMs). CMs can be obtained through invasive surgery (hearth biopsy) or by growing them from human stem cells.

Cardiomyocytes can be differentiated from human embryonic stem cells. This has ethical and practical problems of obtaining the cells from human embryos. Another stem cell type that can be used is human induced pluripotent stem cells (hiPSC). HiPSC are reprogrammed from adult human cells into a pluripotent state. This gives the advantage of being able to gather cells from adults which increases the supply of the cells and circumvent the ethical problems associated to embryonic stem cells. Another advantage is that the hiPSCs have the same genome as the donor. (Takahashi et al. 2007) This allows the production of patient and disease specific cells that can be used to study different diseases and create disease specific models.

The use of hiPSC-derived cardiomyocytes (hiPSC-CMs) has challenges. When cultured in normal *in vitro* conditions, hiPSC-CMs do not express the structural and functional properties of adult CMs (Rao et al. 2013, Yang, Pabon & Murry 2014). To make the drug screenings and disease models accurate, the hiPSC-CMs should resemble adult CMs as closely as possible.

The heart group at BioMediTech uses hPSC-CMs to study and create models that can be used for drug testing. The Heart group has tried topographical methods to induce structural maturation to make the hiPSC-CMs more adult like. One project was to use PET textiles (Junnila 2016). Junnila established that hiPSC-CMs grown on PET textiles had improved structural orientation compared to hiPSC-CMs grown on flat surfaces. However, the number of cells found on the textiles was lower than on flat surfaces. Whether this was due to poor attachment or detachment of the cells remained unknown. It was also considered that the textile structure could prevent the detection of the cells.

This thesis is a continuation to Junnila's thesis (Junnila 2016) with the purpose of determining if the cell attachment could be improved by using different coatings on the textile. As the larger goal is to increase the maturation of the hPSC-CMs, the structural properties of CMs grown on differently coated textiles were carefully determined. This was done to find a coating material that optimizes both the number of viable cells and the

structural maturation of the cells. Both the samples and the growth wells where the samples were incubated were studied to determine whether the problem is in attachment or in detection methods.

2. LITERATURE REVIEW

2.1 Stem cells

Stem cells are undifferentiated cells that can divide and self-renew indefinitely or can differentiate into specialized cell types. Stem cells are capable of symmetrical cell division producing two identical copies of the original cell and asymmetrical cell division that produces a cell that resembles the original cell and another cell that starts to differentiate towards certain pathway. (Wolbert et al. 2007)

There are several kinds of stem cells with different differentiation capacity. A fertilized egg is considered totipotent. Totipotent stem cells can form all cell types of developing organism and extra embryonic structures like placenta, umbilical cord and fetal membranes. In mammalian embryogenesis, totipotent cells are found until the embryo reaches the eight-cell morula stage. After that all cells specialize to extra embryonic elements or to form an organism. The stem cells that can differentiate into any cell type in an organism are called pluripotent stem cells. (Wolbert et al. 2007)

In the embryo development, the pluripotent stem cells start to differentiate towards certain cell types and start to lose their capacity to differentiate into alternative cell types. Multipotent stem cells can produce only a few different cell types. The cell types are usually found in the same tissue where the stem cell resides. Multipotent stem cells are also called tissue specific stem cells. In addition to embryos and fetuses, multipotent stem cells can be found in adult tissues. Lastly unipotent stem cells can only self-renew or differentiate into one type of cell. (Wolbert et al. 2007)

2.2 Human induced pluripotent stem cells

Induced pluripotent stem cells (iPSC) were first introduced by Takahashi and Yamanaka 2006. They managed to produce pluripotent stem cells from mouse somatic cells by introducing four factors, Oct3/4, Sox2, c-Myc and Klf4 (Takahashi, Yamanaka 2006). Pluripotent stem cells from adult human dermal fibroblasts were produced using the same four factors (Takahashi et al. 2007). By this process the production of human induced pluripotent stem cells (hiPSC) became possible. HiPSC provide certain advantages. They can be produced from adult cells and thus they do not have same ethical and practical problems as embryonic stem cells and they can be considered as nearly unlimited source (Jukes et al. 2008). Also, as they can be produced from cells harvested from patients, they can be used to study patient specific diseases. This helps in disease modeling, and in future may allow patient specific treatments. (Khan, Lyon & Harding 2013)

2.3 Cardiomyocytes and the human heart

The human heart is a muscular pump which maintains blood pressure and circulation. The heart consists of four chambers. The two upper chambers are called atria and they collect blood. The lower chambers are called ventricles which are stronger and function as blood pumps. The chambers are divided into two halves, right and left. The right atrium collects the blood from the body which is then pumped to the lungs by the right ventricle. The oxygen richened blood is then collected into the left atrium and is then pumped to the rest of the body by the left ventricle. The blood flows only in one direction in the heart. The direction is maintained by four valves that prevent the blood from flowing into the other direction. The walls of the heart consist of three layers. The outer layer is called pericardium. The middle layer is the myocardium which is where the contraction happens. The inner most lining is endocardium. (Weinhaus, Roberts 2005)

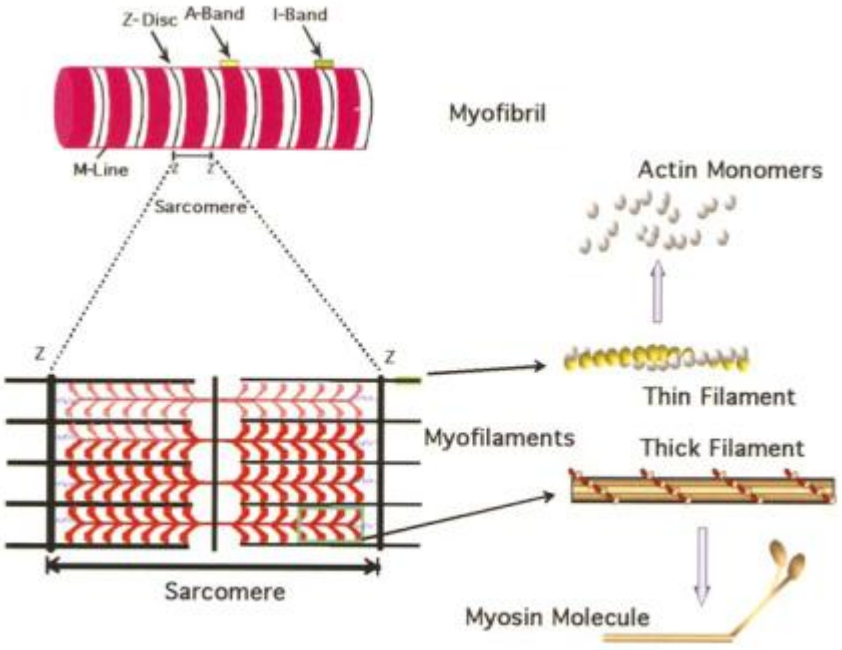

Figure 1. *Protein structure of the parts causing contractions. Cardiomyocytes contain myofibril bundles that run across the cell. Myofibrils consist of smaller contractile units called sarcomeres. The actin and myosin are arranged into filaments and their interaction is the basis of muscle contraction (Barnett 2005).*

The myocardium consists of cardiomyocytes (CMs) and connective tissue. The CMs can vary in size and shape, but in general they are ~50-200 μm along the force generation axis and ~10-40 μm in width. The contractile proteins within CMs are organized into sarcomeres (Figure 1). Sarcomeres function as contractile units and they are bordered in each end by a Z line which is a protein matrix composed primarily a-actinin. In each sarcomere, there is an interdigitating lattice of thin and thick filaments. The thin filament consists of polymeric assembly of globular protein actin subunits, and they also contain regulatory proteins tropomyosin (Tm) and troponin (Tn). The thick filament consists of

protein myosin. The contraction in sarcomeres happen in several steps. First, myosin can bind adenosine triphosphate (ATP), but it cannot use the energy released during the hydrolysis of ATP as it is inhibited by Tm and Tn. The inhibition of the Tm-Tn complex is released by calcium binding to troponin. This allows the energized myosin to attach to the thin filament. Actin from thin filament catalyzes the release of adenosine diphosphate (ADP) and inorganic phosphate, and the myosin head goes through conformational change while it is bound to actin. The change pulls the thin filament past the thick filament which causes contraction. Myosin can then rebind to ATP which allows the detachment of actin and myosin. The hydrolysis of ATP starts a new contraction cycle. (Barnett 2005)

To function properly, the atria and the ventricles have to contract one after another. The heart beat is controlled through cardiac conduction system. The sinoatrial node works as the pacemaker of the heart. The cells in the node have spontaneous depolarization that generate the cardiac rhythm, which is modulated by sympathetic and parasympathetic intervention. There are several pathways that conduct the depolarization at the right time to the correct part of the heart. Normally the contraction originates from sinoatrial node and then propagates through both atria. The atrial depolarization spreads to atrioventricular node, goes through bundle of His and then to the Purkinje fibers which make up the left and right branches. This causes all ventricular muscles to become activated. The different pathways are presented in Figure 2. (Laske, Iaizzo 2005)

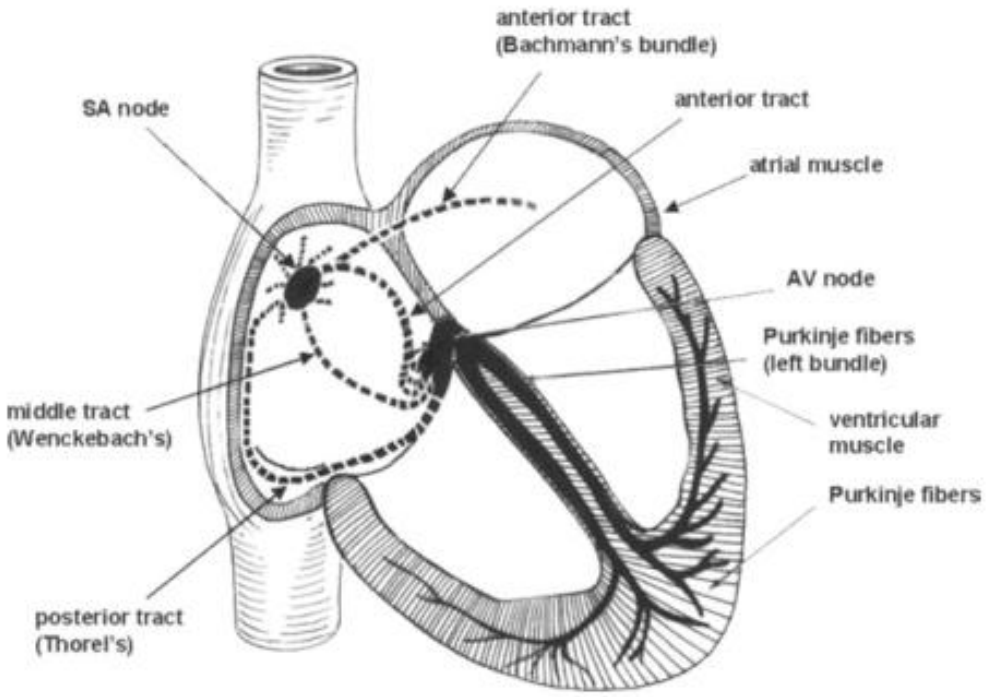

Figure 2. *The conduction system of human heart. The contraction starts at sinoatrial (SA) node and goes through the pathways to have correct parts of the heart contract at the right time (Laske, Iaizzo 2005).*

2.4 Human induced pluripotent stem cell derived cardiomyocytes

Human induced pluripotent stem cell derived cardiomyocytes (hiPSC-CM) can be produced by various methods. First is to differentiate hiPSCs to CMs through embryonic bodies (EBs), second is to co-culture them with mouse endodermal-like cells (END-2) and lastly the differentiation can be driven by defined growth factors on monolayer.

EBs can differentiated spontaneously from hiPSC. The pluripotent stem cells are first dissociated into small cell clusters. The cell clusters are then allowed to form aggregates in suspension after which the EBs are plated on culture plates. (Kurosawa 2007) There are several culturing methods to form EBs, like hanging drop culture, suspension culture in bacterial-grade dish, methylcellulose culture, spinner flask and round-bottomed 96-well plate (Kurosawa 2007). There are also other methods for EB formation. The forced aggregation method uses centrifugation to force the formation of EBs (Burridge et al. 2007, Ng et al. 2005). The advantage of this method is better control over cell numbers and EB sizes (Burridge et al. 2007).

In the END-2 differentiation method, the hiPSC are co-cultured with mouse endodermal-like cells (END-2), especially in the absence of ascorbic acid and serum. (Mummery et al. 2003, Passier et al. 2005). The differentiation factors are secreted by the END-2 cells. This means that END-2 conditioned medium can be used for cardiomyocyte differentiation instead of co-culturing (Graichen et al. 2008). The mechanism or the specific factors by which END-2 cells induce differentiation are still unclear. Testing shows that END-2 cells clear insulin from the medium which is believed to have an impact in the process (Xu et al. 2008).

The differentiation can be controlled through the use of specific growth factors. High-density undifferentiated monolayer of hPSC on Matrigel coated surface can be differentiated into cardiomyocytes. This is done by combined application of activin A and BMP4. Addition of Wnt3a in the early phase of activin A/BMP4-directed cardiac differentiation, with inhibition of Wnt/β-catenin in later stages, increases cardiac differentiation. Depending on the molecule inhibiting the Wnt-pathway the amount of ventricular cardiomyocytes compared to atrial-like cardiomyocytes can be changed. (Acimovic et al. 2014) EB formation can also be guided by using growth factors. EB differentiation has been achieved with use of activin A, BMP4, bFGF, VEGF and Dkk-1. After plaiting the EBs grown with these factors, a population with over 50% of beating CMs was achieved (Yang et al. 2008).

2.5 Characterization of differentiated cardiomyocytes

There are several ways to characterize differentiated CMs. They can be characterized through functional and structural analysis, cardiac marker expression, electrophysiology, and excitation-contraction coupling.

The most apparent property of successfully differentiated hPSC-CMs is their ability to spontaneously contract in the culture (Mummery et al. 2003, Kehat 2001). A structural marker for CMs is that at first the myofibrils are randomly situated throughout the cytoplast, but in later stages of the differentiation, the sarcomere structures start to become more organized (Snir 2003, Kehat 2001).

The differentiated CMs have several cardiac markers and they are expressed differently at different phases. The gene expression of beating hPSC-CMs follows the pattern of early embryogenesis. First up-regulated genes are primarily mesodermal, like Brachyury T (Beqqali 2006). The differentiation then continues with the expression of regulatory factors like Islet-1, Mesp 1, GATA-4, Nkx2.5 and Tbx6. (Graichen et al. 2008, Yang et al. 2008) Other markers that can be used as maturation markers are cardiac troponin T, cardiac troponin I, myosin proteins and cardiac a-actinin (Kehat 2001, Mummery et al. 2003).

Electrophysiological properties are important to CMs. For differentiated beating cells to spontaneously contract and have spontaneous action potential activity, they have to have cardiac structural proteins and ion currents. (Kehat 2001, Mummery et al. 2003) If the spontaneous action potentials of differentiated CMs are compared to human neonatal or ventricular CMs, the differentiated CMs have relatively positive maximum diastolic potential and the maximum rise rate of action potential is relatively slow (He 2003).

The elevation of intracellular Ca^{2+} is linked with contraction of a CM (Bers 2013). This means that the calcium transients during contraction and relaxation can be used to study the functionality of cardiomyocytes.

2.6 The extracellular matrix

The extracellular matrix (ECM) is a complex component found in all tissues. The ECM is a meshwork of extracellular collagens, proteoglycans and adhesion proteins, and other molecules like growth factors, chemokines and cytokines. The ECM has several important functions, both structural and biological. It provides support, tensile strength and scaffolding for cells and tissues; works as boundary between different cell types and works as a storage for growth factors, cytokines and chemokines. The ECM also affects cell polarity, cell adhesion, cell morphology and differentiation, cell migration, proliferation and even apoptosis. The amount of different ECM components vary depending on the tissue. For example, cartilage ECM is enriched in large proteoglycans

and collagen II, which allows increased compression resistance. Basement membrane matrices are enriched in the glycoproteins, laminin, entactin/nidogen and collagen IV with lesser amounts of proteoglycans and growth factors. The basement membrane matrices separate different tissue types and have other functions like molecular filtering in kidneys. (Kleinman, Philp & Hoffman 2003)

The ECM molecules found in cardiac tissue include hyaluronan, fibronectin, fibrillin, proteoglycans and collagens. Glycosaminoglycans (GAGs) are polysaccharide chains with repeating amino sugar and uronic acid disaccharide units. The most abundant GAG in developing heart is hyaluronan (HA). HA is part of the matrix that provides hydrated environment and facilitates cellular proliferation. HA is present in epicardial mesenchyme and the interstitial space surrounding the cardiomyocytes of the myocardial structures. (Lockhart et al. 2011)

Proteoglycans consist of core protein with associated GAG sidechains. There are four classes of GAGs in heart, hyaluronan, chondroitin sulfate, heparin sulfate (heparin) and keratin sulfate. Heparin sulfate proteoglycans have a crucial role in heart development and homeostasis. The heparin sulfate chains are able to bind multiple growth factors and cytokines which are important to cardiac development, including VEGF, BMPs, FGFs and TGFβs. (Lockhart et al. 2011)

Another large ECM protein family found in the heart is collagen. Collagen types I, III, V and VI are found in the ventricular myocardium, the developing AV valves and chordae tendineae. Collagens II, IV, XI and XIII are found in the developing valve structures and tendinous apparatus. There are also two non-fibrillar collagens, type XV and XVIII, expressed in both developing and adult heart. (Lockhart et al. 2011)

Other important parts of cardiac ECM are proteases, fibrulins, fibronectin; which is a multi-domain protein that interacts with multiple integrins, heparin sulfate proteoglycans, collagens and fibrins to mediate cellular behavior; and fibrillin which forms microfibrils with other ECM molecules such as elastin. (Lockhart et al. 2011)

2.7 Extracellular matrix proteins as coating material

As previously discussed the extracellular matrix not only provides structure and support for cells but also important biological functions such as cell adhesion, migration and proliferation and it binds other important molecules like growth factors (Kleinman, Philp & Hoffman 2003). To improve cell culturing conditions *in vitro* it is important that the cells get the same kind of continuous feedback from their surroundings as they would in their natural environment. To achieve this, the growth surfaces can be coated with ECM proteins, parts of the proteins, or with biomimetic materials with similar structures to natural ECM proteins. (Patterson, Martino & Hubbell 2010) A structure that is well recognized by cellular receptors is the arginine-glycine-aspartic acid peptide sequence.

The sequence can be found in ECM proteins fibronectin, vitronectin and collagen. This peptide by itself can make non-adhesive surfaces into adhesive ones for cells. The sequence can be implemented as a part of the proteins or as short peptide sequences that can be synthetized. As large proteins fold randomly over a surface, the cell attachment sites might not be as readily available as they are with smaller peptide chains. (Shin, Jo & Mikos 2003) Cells have many receptors for different amino acid sequences and other ECM proteins have other peptide sequences for attachment. But as mentioned previously ECM proteins are multifunctional, so having only the binding sites might not have the same effect as the whole protein. The signaling pathways are usually made of multiple components, so the coating should consist of suitable combination of ECM proteins and growth factors. (Shin, Jo & Mikos 2003, Stevens, George 2005) The ECM coating will also form nano- and microscale topographical features like grooves, ridges and nanofibers. These topographical features affect cell behavior, proliferation, motility, cell shape, and protein production (Stevens, George 2005).

Different tissue types have different types of ECM (Kleinman, Philp & Hoffman 2003). This means that different cell types have their own preferences for ECM coatings both biochemically and physically. To have optimal culturing results it is important to find the right kind of combination for the cultured cell type. The ideal coating should be determined for each cell type and to do that it is important to understand the different signaling pathways of different cells and how they react to their surroundings. (Brandl, Sommer & Goepferich 2007, Stevens, George 2005)

2.8 The attachment of extracellular proteins to surfaces

The attachment of cells to surfaces in liquid environment consists of three major stages. First the water molecules come to contact with the surface. Depending on the hydrophilicity of the surface, the water molecules react differently. If the surface reacts easily, the water molecules can dissociate and the surface will be covered with OH-groups. If the surface does not dissociate the water molecules it can be either hydrophilic or hydrophobic. If the bonds between the surface and the water molecules are stronger than hydrogen bonds in ice the material is still hydrophilic and if the bonds are weaker, the material is hydrophobic. The protein adsorption is more irreversible on hydrophobic surfaces and the proteins have a tendency to denature. On the other hand, too hydrophilic surfaces may inhibit protein adsorption. The topography and the shinelectrical charge of the surface also affects the attachment. In the second phase, larger molecules like proteins interact with the surfaces. Water soluble biomolecules always have attached water molecules. Most of interactions are between the water layers of the molecules and the surface. The water interactions determine how the proteins react to the surface. The protein can attach, fold, denature or orient itself. On hydrophilic surfaces the proteins attach via hydrophilic parts and on hydrophobic via hydrophobic parts of the structure. The attachment of the protein may vary. They can attach uniformly across the surface,

form isolated clumps or they might not even attach to the surface at all. In the third phase, cells react with the proteins and water molecules on the surface. The cell receptors bind with available parts of the proteins, attaching the cells to the surface through the proteins. (Ma, Mao & Gao 2007, Kasemo 2002)

When using ECM proteins to coat a surface they are usually irreversibly adsorbed. They usually stay put on the surface and do not gradually move inside the bulk material. The exact reactions depend on the material and the proteins involved. The reactions are determined by the adsorption kinetics, strength of the bonds and the folding of the proteins. (Kasemo 2002, Shin, Jo & Mikos 2003) Depending on the surface substrate the penetration may vary. On rigid solids like glass, the coating might penetrate only few nanometers, whereas on polymers capable of swelling the coating might penetrate micrometers. (Ventre, Causa & Netti 2012).

2.9 Extracellular coating materials

Collagen is the most abundant (~30 %) protein in the body. It is also the largest component of the ECM. It serves as tensile strength provider for tissues and organs. Collagen can be found across many tissues and it forms the structural framework of connective tissues like bone, tendons and dermis. There are at least 28 different vertebrate collagens. (Muiznieks, Keeley 2013) The collagens are structurally heterogeneous, which allow them to contribute in various functions like cell adhesion and migration, tissue repair, molecular filtration and tumor suppression. (Kadler et al. 2007) The surface of collagen fibrils is important for interactions with matrix macromolecules (Muiznieks, Keeley 2013). Collagen has been used to grow mesenchymal stem cells in 3D poly-L-lactide scaffolds. Collagen coating increased protein adsorption and improved adhesive properties of the scaffolds. The use of dynamic pump driven coating procedure increased the number of mesenchymal stem cells in the culture compared to coating procedure of static incubation overnight. (Rodina et al. 2016)

Gelatin is a modified version of collagen. Gelatin is produced from mammalian bone and skin or from fish skin with thermal hydrolysis. Gelatin is a polypeptide with gelling and melting temperature below +35 °C. In addition to cell culturing and regenerative medicine research it is used a lot in food and pharmaceutical industry. In cell culturing it is used to produce a thin, somewhat uniform layer. There can be some globular aggregates present in the coated surface. (Wang, Yang & Regenstein 2008) When using gelatin it will form a gel and have fibrillary structure in higher than 1 % concentrations. The structure and topography of gelatin coating is somewhat difficult to examine as the gel loses some of its characteristics when it dries, which can change its shape (Wang, Yang & Regenstein 2008, Yang et al. 2007). Gelatin with 0.1 % concentration has been the standard coating material for cell culture in our laboratory (Kujala 2012, Junnila 2016). To improve the attachment of gelatin to a polymer, the polymer can be chemically modified. The

modification material cannot be harmful to the cells. Dopamine has been successfully used to increase the amount of gelatin attaching to polyethylene terephthalate (PET). The exact reactions are not well known, but the amount of gelatin was increased with chemical binding. (Giol et al. 2015)

Laminins are ECM proteins with multidomain structure. The structure consists of three polypeptide chains. Laminins were found from epithelial basement membrane in contact with collagen type-IV and they are structurally important part of the ECM (Timpl et al. 1979). The tertiary structure of laminin is cross-like with globular and rod-like domains extending into 4 arms from the middle point. This helps it to reach binding sites of different cells and ECM molecules (Beck, Hunter & Engel 1990). Laminins have several functions. They bind skeletal muscle's cytoskeleton to other ECM proteins and they bind agrin in neuro-muscular junctions. Laminins also have several EGF-like repeat units that work like growth factors. They polymerize into sheets that form networks with collagen, affecting the mechanical properties of the basement membrane (Aumailley et al. 2005). Laminins have been shown to promote neural growth in vitro (Luckenbill-Edds 1997) and they have been used to grow hESCs feeder-free (Xu et al. 2001). There are differences between laminins when using them as coating material. In myogenic cell culture, laminin 521 was superior in short-term and long-term culturing compared to laminin 111, laminin 211 and gelatin. Laminin 521 was also comparable to Matrigel in short term studies and provided more consistency in the long-term studies. Additionally laminin 521 was human origin making it more suitable for cell therapy development. (Penton et al. 2016) Laminin coatings have also been used to enhance osteogenic biomarker expression and osseointegration (Javed et al. 2016), and to make endothelial cell differentiation from hPSCs more efficient (Ohta et al. 2016).

Fibronectins are glycoproteins found in the ECM. They are found in most tissues and are considered important for the mechanical properties of the ECM. The differences between fibronectin molecules are smaller than the differences between laminins. For this reason they are usually called fibronectin without distinguishing the molecular domains. Fibronectins molecular structure is asymmetric, elongated and flexible. It consists of small and compact globular units. (Hynes, Yamada 1982) The globular units can function as individual fragments as long as they fold into right shape. Some of the modules are important for cell binding as they form easily reachable loops for other molecules and cells. Other modules work as binding sites for collagen and gelatin. (Potts, Campbell 1996, Wilson et al. 2004) Fibronectin has been used to grow mesenchymal stem cells on PDMS surface. The growth densities were comparable to tissue culture polystyrene controls (TCPSs). The advantage of fibronectin coated PDMSs is that the cell sheets could be easily separated from the surface with the use of oil. (Juthani et al. 2016)

Matrigel is a commercial product that contains ECM proteins, extracted from basement membrane. Matrigel is produced in Engelberth-Holm-Swarm mouse tumors which have

an abundance of basement membrane. The tumor consists of different biomolecules. The highest concentrations are laminin-1, collagen type-IV, perlecan and enactin which are ECM proteins. There are also other molecules like proteases, growth factors (EGF, FGF, TGF-β) and other proteins. Matrigel is also available in growth factor reduced form. (Kleinman, Martin 2005) The physical properties of Matrigel have also been studied. Matrigel forms topographical features such as elevations, pores and fibers with dimensions ranging roughly from 50 nm to 200 nm (Abrams et al. 2000). The elastic modulus ranges from 400 to 1000 kPa, which resembles the elastic modulus of softer tissues. There is lot-to-lot variation and the stiffness also varies in different temperatures. (Soofi et al. 2009) Matrigel can be used in many applications. It has been used to grow hESCs feeder-free (Xu et al. 2001). There are studies that have shown that Matrigel can preserve the pluripotency of iPSC (Oberwallner et al. 2014), but also studies showing that Matrigel promotes differentiation and maturation of cardiomyocytes (Burridge et al. 2012, Zhang et al. 2012). Oberwallner et al. 2014 presented that the difference could be due to different source of the iPSCs (murine vs human) and the difference in growth factors. Matrigel has also been used for endothelial cell tube assays, 3D culture of cells, invasion assays and spheroid assays (Benton et al. 2014).

Geltrex is a commercial ECM protein mix, extracted from basement membrane. Like Matrigel it is produced in murine Engelberth-Holm-Swarm tumor. The major components include laminin, collagen IV, entactin and heparin sulfate proteoglycan. As mixture of ECM molecules Geltrex provides physical support as well as other cellular function like proliferation, adhesion, migration, differentiation and polarization. Geltrex can be used to culture several cell types including iPSCs. (Geltrex® LDEV-Free 2014) Geltrex has been used for *in vitro* culture of primary epithelial cancer cells. The results were comparable to feeder layer grown tumor cells. However, the use of Geltrex was simpler than the use of feeder layer. (Janik et al. 2016) Geltrex has also been used to grow mammary epithelial cells (Shandilya et al. 2016) and human embryonic stem cell-derived beta-like cells (Massumi et al. 2016). Geltrex has been shown to preserve the pluripotency of iPSC similarly to Matrigel (Oberwallner et al. 2014).

2.10 Approaches to improve cell maturation

The problem with hiPSC-CMs is that they are more fetal than adult-like. There are several approaches to increase the maturity of the hPSC-CMs. Biochemical approach includes the use of growth hormones and adrenergic stimulation. Molecular biology approach uses overexpression of cardiac specific ion channel and microRNA to create changes in electrophysiology and calcium handling. The bioengineering approaches are to use the materials topography and stiffness; mechanical and electrical conditioning; and systems that improve nutrient delivery. The assessment of maturation is done through several methods. The morphology of the cell is important maturation marker and it includes the shape and size of the cell, the sarcomere orientation, presence of T-tubules and the

alignment of cells. Another way to assess the maturation of the cells is through molecular assays, like gene expression analysis, comparing how closely the gene expression matches that of adult CMs. The functional assays are also important as they tell how closely the cells work like adult CMs. The functionality can be tested through calcium transients, electromechanical coupling, contraction and electrophysiology. (Tzatzalos et al. 2016) The different approaches to increase maturation and to assess it are presented in Figure 3.

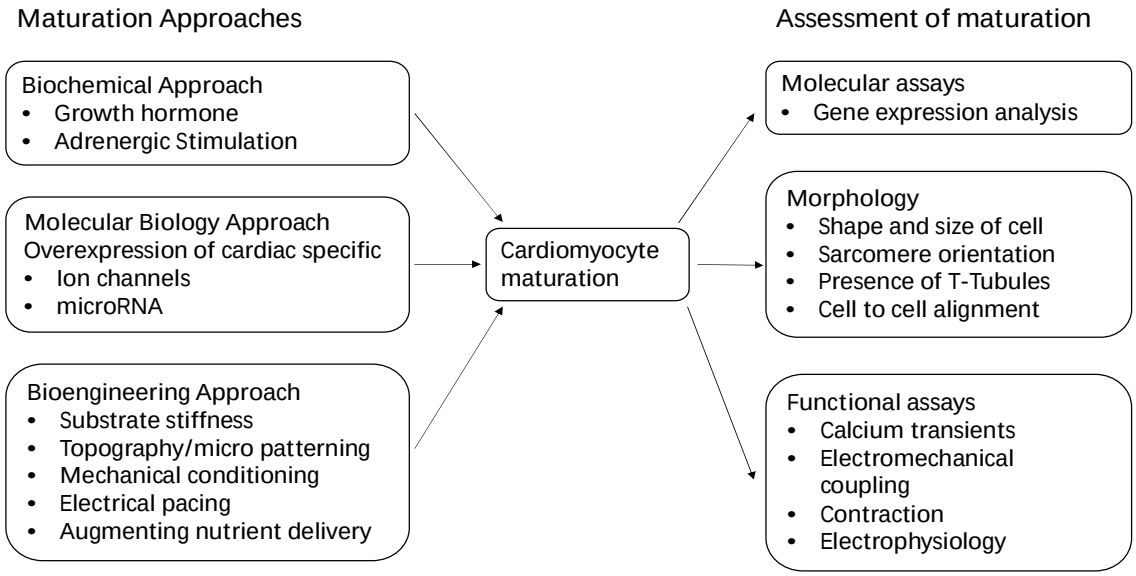

Figure 3. *Maturation and assessment approaches to the maturation of cardiomyocytes (Adapted from Tzatzalos et al. 2016).*

The use of topography has been a common way to try improving cell alignment and structural maturity. One approach to topography is using fibers and wires as growth platforms (Han et al. 2016, Khan et al. 2015, Nunes et al. 2013). In a study using Matrigel-coated anisotropic and isotropic polycaprolactone (PCL) fibrous scaffolds, it was found that anisotropic scaffold experienced higher orientation. The difference in functional properties was not as clear. The hPSC-CM grown on anisotropic fibrous scaffolds had highest expression of genes that encode sarcomere proteins, ion channels and proteins affecting calcium handling. However, their calcium transient kinetics were slower than cells grown on TCPs. This indicates that the electrospun anisotropic fibrous scaffolds have only limited effect on the maturation of hPSC-CMs. It was concluded that the method was shown to increase alignment but other methods should be used in combination to create a suitable method to increase the maturation of hPSC-CMs. (Han et al. 2016) In another test highly aligned polylactide-co-glycolide (PLGA) nanofiber scaffolds were used to align hiPSC-CMs and they were compared to ones cultured on standard flat culture plate (Khan et al. 2015).The fibers were made with electrospinning. The cells grown on the nanofibers demonstrated symmetrical alignment with the fibers they were grown on which was significantly greater than the alignment on flat surface. The nanofiber cultured hiPSC-CMs had well organized myofibrils in contrast to the flat

surface cultured ones. When testing mRNA levels of a-actinin and Troponin-I, no differences could be found between nanofiber cultured hiPSC-CMs and flat surface grown. The nanofiber grown cells had higher calcium cycling and beat rate than flat surface grown. (Khan et al. 2015)

Other morphology approaches to maturation include the use of microgrooves (Rao et al. 2013), high-resolution photolithography and microcontact printing (Salick et al. 2014) and multiscale biomimetic topography (Luna et al. 2011).The microgrooves were found to increase the alignment of the cells and improve the Ca^{2+} regulation, but they did not show improvement in action potentials, protein localization or gene expression (Rao et al. 2013). The dimension and scale of the topography affects the orientation of CMs. Patterns with varying length to width ratios have been tested. It was detected that the width of the growth lane is more important than the overall ratio. The patterns widths between 30 µm to 80 µm produced the most organized sarcomere structures and nuclei orientation (Salick et al. 2014). To test multiscale biomimetic topography, 20 nm to 10 µm wrinkles were made to PDMS microchips. The idea was to mimic the heart's anisotropic and multiscale architecture. The CMs on wrinkled substrates had increased alignment compared to non-wrinkled samples (Luna et al. 2011).

There are also methods that do not include topography. These include mechanical load (Tulloch et al. 2011), electrical stimulation (Radisic et al. 2004) and co-culturing with other cells (Tulloch et al. 2011, Ravenscroft et al. 2016). It was found out that static and cyclic stress increase cardiomyocyte alignment. (Tulloch et al. 2011). The use of electrical stimulation mimicking the signals in native heart has been detected to induce cell alignment and coupling, and also to induce the development of long well aligned sarcomeres. (Radisic et al. 2004) The transient Ca^{2+} amplitudes, the spontaneous contraction rate and the contractile function of hESC-CM was increased when co-cultured with cardiac non-myocyte cells (Ravenscroft et al. 2016). No improvement in CM orientation, the transient Ca^{2+} amplitudes, the spontaneous contraction rate or the contractile function was detected when co-culturing with endothelial cells or fibroblast from non-cardiac tissues (Tulloch et al. 2011, Ravenscroft et al. 2016).

There have also been studies using multiple different methods to increase maturation. Nunes et al. 2013 combined several methods to maturate hPSC-CMs on what they called "biowire". They seeded the hPSC-CM with supporting cells like fibroblasts, endothelial cells and smooth muscle cells into a template channel of PDMS around a surgical suture in type I collagen gel. After the cells had attached to the collagen matrix the "biowire" was removed from the PDMS template. They detected that the biowire beat synchronously and spontaneously. In addition, the biowires could be paced electrically to test the effect of electrical stimulus on the maturation of hPSC-CMs on the biowire. They detected well defined Z discs and myofibrils in both electrically stimulated wires and non-stimulated wires. The biowires with high-frequency stimulation displayed higher Z disc

alignment than non-stimulated. The sarcomere organization in the stimulated wires was closer to mature cells than with non-stimulated wires. They also came into conclusion that the electrical stimulation promoted electrophysiological maturation of the cells. (Nunes et al. 2013)

2.11 Aims of the study

There were three main objectives in the present study.

1. Determine a suitable coating material to improve the attachment of hiPSC-CMs to PET textile structure.
2. Determine how the different coating materials affect the structural maturation hiPSC-CMs.
3. Determine if the textile or the coatings have detrimental effects on analysis methods.

In a previous study (Junnila 2016) it was shown that the PET textile increases the structural maturation of the hiPSC-CMs. Only gelatin coating was used in that study and the number of cells found on the textile samples was low compared to control samples. The first goal was to increase the attachment of cells. Five different coatings were used in this study to find an optimal coating that improves the attachment of hiPSC-CMs to PET textile without compromising the increase in structural maturity. The second goal of the study was to find out if the coating material itself affects the structural maturation. The third goal was to see if the lack of detected cells in the previous study was due to low attachment or because the textile structure prevents the detection of the cells.

3. MATERIALS AND METHODS

3.1 Sample materials

There were two textile materials used in this study. The main material was polyethylene terephthalate (PET). Two different kinds of weave patterns were used for PET textiles. The second material was poly-L/D-lactide (PLDLA). The textile structures can be seen in Figure 4.

3.1.1 Polyethylene terephthalate

The standard textile sample in the present study was the commercially produced PET-textile from Inka Oy (Killinkoski, Finland). The textile was colorless with textured weft yarn. The textile was heat treated at Tampere University of Technology (TUT). The structure of the textile can be seen in Figure 4 A.

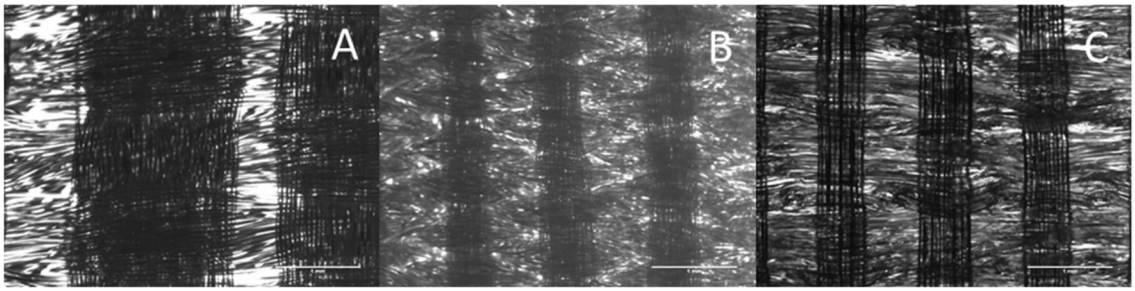

Figure 4. *The different textile structures imaged on Zeiss Axio Vert.A1 microscope with AxioCam MRc5 camera. All images are taken on 5x magnification. The scale bar is 1 mm. A) is the commercial colorless PET from Inka Oy, B) is the blue plain weave derivate PET from TUT, C) is the transparent plain weave PLDLA 96/4 from TUT.*

The other PET-textile samples were also manufactured of PET multifilament yarn by weaving. These textiles were made in TUT and color of the material was blue. The material was used, because it was easily available. The weaving pattern was plain weave derivative. The PET yarns had a fineness of 78 dtex and each yarn composed of 24 filaments. The warp density of the woven textile structure was ~155 yarns/cm and there were 6 warp yarns per reed dent. The structure of the textile can be seen in Figure 4 B.

3.1.2 Poly-L/D-lactide

The other textile samples were made on poly-L/D-lactide copolymer with L/D isomer ratio of 96/4 (PLDLA 96/4) yarns. Cross-section of all the filaments in the yarn was star-shaped. The weaving pattern was plain weave and the warp density of the manufactured

textile was ~85 filaments/cm. The textiles were manufactured at TUT and they were transparent. The structure of the textile can be seen in Figure 4 C.

3.1.3 Controls

The control samples were 13 mm diameter glass cover slips.

3.2 Coating materials

Five different coating materials were used. Gelatin, collagen, Matrigel, Geltrex and dopamine bound gelatin. For all coatings, the textiles and the coverslips (control) were washed with 70 % ethanol and left to dry before the coating. The purpose of the coatings was to create a thin layer on the textile to increase attachment without compromising topography. Two parallel samples were always used to reduce the amount of random variation.

3.2.1 Gelatin

The gelatin used to coat the textiles was Sigma G1890-100g (Sigma-Aldrich), which is gelatin type A from porcine skin in powder form. The gelatin is a heterogeneous mixture of water-soluble proteins and the Sigma G1890-100g consists of 70-90 % of protein. The gel strength is ~300 g Bloom. The gelatin was dissolved into 1xPBS to make 0.1 % solution. 500 µg of the 0.1 % gelatin was pipetted on the textiles and 150 µg on coverslips. The coatings were incubated for 1 hour in room temperature after which the extra coating was aspirated. The gelatin was chosen as the basic coating method as it has been used for growing cells on cover slips and the concentration is optimized for the cell lines used in the heart groups laboratory.

3.2.2 Collagen

The collagen was type 1 rat tail collagen from BD biosciences (CAT No. 354236). The concentration of the collagen was 3.92 mg/ml. The collagen was diluted into 50 µg/ml with 0.02M acetic acid. The solution was then sterilized through supor membrane. 500 µl of sterilized solution was used to coat the PETs and 150 µl to coat the coverslips. The coatings were left to incubate for 1 hour in room temperature after which the excess material was aspirated. The coatings were washed 3 times with PBS or serum free medium to remove remaining acid.

3.2.3 Geltrex

The coating material was Geltrex® LDEV-Free Reduced Growth Factor Basement Membrane Matrix (CAT No. A1413202) from Life technologies. The major components

include laminin, collagen IV, entactin, and heparin sulfate proteoglycan. Geltrex is stored in smaller volumes in -20ºC. Before using, Geltrex was thawed on ice in a refrigerator. During use Geltrex was kept on ice and cold pipettes were used to prevent premature gelling. When using Geltrex, it was diluted into KO-DMEM medium in ratio of 1:100. 500 µl of diluted Geltrex was pipetted on textiles and 150 µl on coverslips. The samples were left to incubate for 1 hour in 37ºC. After that the excess material was aspirated and the coatings were ready for use.

3.2.4 Matrigel

The coating material was Corning Matrigel Basement Membrane Matrix Growth Factor Reduced (CAT No. 354260). The major components include laminin, collagen IV, entactin/nidogen, and heparin sulfate proteoglycan. Matrigel is stored in small volumes in -80ºC. Before using, Matrigel was thawed on ice in a refrigerator. During the use Matrigel was kept on ice and cold pipettes were used to prevent premature gelling. Matrigel was diluted into KO-DMEM medium in ratio of 1:100. 500 µl of diluted Matrigel was pipetted on PETs and 150 µl on coverslips. The samples were left to incubate for 1 hour in room temperature. After that the excess was aspirated. The coated samples were then washed with KO-DMEM medium and the coatings are ready for use.

3.2.5 Dopamine bound gelatin

Dopamine hydrochloride (Sigma H8502) was used to crosslink gelatin with the PET fibers. This was done to increase the attachment of gelatin and to prevent the coating from detaching during experiments. The dopamine was dissolved into Tris-HCl buffer. The Tris-HCl buffer solution was prepared from Trizma base (Sigma T1503) into hydrochloric acid (Sigma-Aldrich 258148), pH 8.5. The used dopamine solution was 2 g/l. First, the PET fibers were left to incubate in the dopamine solution for 24 h on a shaking bed at room temperature. The dopamine modified samples were washed with distilled water. After washing the dopamine-modified samples were incubated in Gelatin type A (Sigma-Aldrich G1890) solution for 24 h in 37ºC. The Gel-A solution was 5% (w/v) of gelatin in Tris-HCl buffer. After incubating in gelatin the samples were rinsed and incubated overnight in distilled water at 37ºC to remove any physically absorbed gelatin. The difference in concentration (5% vs 0.1%) and solution (Tris-HCL vs PBS) of the dopamine bound gelatin compared to the gelatin and the gelatin with plasma treatment was due to the coating protocol given for dopamine usage. (Giol et al. 2015)

3.2.6 Plasma treatment

The plasma treatments were made with plasma system type Pico, Model 2, standard system with PCCE control and RIE-electrode. The electrode was type E (stainless steel), the generator was type D (13.56 MHz, 0-100W) and the vacuum pump was Leybold

SC5D. The producer is Diener electronic GmbH (Germany) and the serial number is 113197. The treatments were done to modify the surface properties of the samples to increase the attachment of coatings and cells. The gas used in the plasma treatment was O_2. The treatment was for 2 min in 0.4 mbar pressure with 50W.

3.3 Differentiation and culture of hiPSC-CMs

The cells used were END-2 or small molecule method differentiated cardiomyocytes from hiPSC. The differentiation was done by BioMediTech's Heart group. There were 3 cell lines that were used in the present study, 04602.WT, 00303.LQT1, 00211.LQT1.

There were several media that were used in the differentiation and culturing of the hiPSC-CM that are listed in following Tables 1-3.

Table 1. *EB-Medium.*

38,75ml	KO-DMEM (Life Technologies)
10ml	FBS (Immunodiagnostic, Biosera)
0,5ml	NEAA (Life Technologies)
0,5ml	Glutamax (Life Technologies)
0,25ml	penisilin/strepsin (City-Lab, Lonza)

Table 2. *0% KO-SR hES.*

48,75 ml	KO-DMEM (Life Technologies)
0,5 ml	NEAA (Life Technologies)
0,5 ml	Glutamax (Life Technologies)
0,25 ml	penisilin/strepsin (City-Lab, Lonza)
97,5 µl	β-mercaptoethanol (Life Technologies)
2,8ml	Ascorbic Acid* (Sigma)

*added just before use

Table 3. *10% KO-SR hES.*

43,75 ml	KO-DMEM (Life Technologies)
5 ml	KO-SR (Life Technologies)
0,5 ml	NEAA (Life Technologies)
0,5 ml	Glutamax (Life Technologies)
0,25 ml	penisilin/strepsin (City-Lab, Lonza)
97,5 µl	β-mercaptoethanol (Life Technologies)

3.4 Cell dissociation and plaiting

After differentiating the hiPSC into CMs, the cells were dissociated from the rest of the cell culture. This was done by isolating beating areas from the culture dish. When using END-2 method the beating areas were cut from the other cells with a micro scalpel. When using monolayer method, the beating areas could be separated without the use of scalpel. The areas were collected with a pipette and then moved to a new well. The new growth well had 500 µl of culture medium collected from the original culture wells. After all the beating areas had been collected they were incubated in three buffer solutions; Low-Ca, Enzyme medium and KB medium. The composition of the buffer solutions is presented in Table 4. First the culture medium was removed and replaced with 0.5 ml of Low-Ca buffer. The excised tissue was washed for 30 min at room temperature after which the Low-Ca was removed and 0.5 ml of Enzyme medium was added. The tissue was left to incubate in the second buffer for 45 min in 37ºC while 10 µl of glucose was added to 0.5 ml of KB medium. The Enzyme medium was then replaced with the KB medium and the tissue was left to incubate for one hour in room temperature. The KB medium was then replaced with EB medium. The tissue clumps were resuspended by pipetting then up and down against the bottom of the dish to break down the clumps. The pipetting had to be done several times to obtain single CMs. The resuspension was a delicate process as too rough execution could damage the cells. 50 µl of the cell suspension was plated on each sample. When using more than 1-2 beating area per sample the cell suspension given to control cover slips was diluted to prevent them from growing confluent. The samples were then incubated for 30-45 min in 37ºC. 650 µl of EB medium was added to all samples and they were then left in incubator.

Table 4. *The composition of buffer solutions. Buffers should be filtered for sterilization and can be stored in -20ºC. *The glucose of buffer 3 (KB) should be added just before using to avoid precipitation.*

	Low-Ca	**Enzyme**	**KB**
NaCl	12 ml (1 M)	12 ml (1 M)	-
$CaCl_2$	-	3 µl (1 M)	-
K_2HPO_4	-	-	3 ml (1 M)
KCl	0.54 ml (1 M)	0.54 ml (1 M)	8.5 ml (1 M)
Na_2ATP	-	-	2 mmol/l
$MgSO_4$	0.50 ml (1 M)	0.50 ml (1 M)	0.50 ml (1 M)
EGTA	-	-	0.1 ml (1 M)
Na Pyruvate	0.50 ml (1 M)	0.50 ml (1 M)	0.50 ml (1 M)
Glucose	2 ml (1 M)	2 ml (1 M)	2 ml (1 M)*
Creatine	-	-	5 ml (0.1 M)
Taurine	20 ml (0.1 M)	20 ml (0.1 M)	20 ml (0.1 M)
Collagenase A	-	1 mg/ml	-
HEPES	1 ml (1 M)	1 ml (1 M)	-
pH correction	NaOH	NaOH	-
pH	6.9	6.9	7.2

3.5 Staining and imaging

For imaging purposes, the samples were stained with live/dead kit and/or immunoflurescence protocol.

3.5.1 Live/dead

Live/dead staining was done by using L3224 LIVE/DEAD® Viability/Cytotoxicity Kit for mammalian cells, Molecular Probes, Inc, Invitrogen. The fluorescent dyes are Calcein

AM (C-AM) which colors live cells and can be seen as green on 488 nm wavelength and Ethidium homodimer-1 (EtHD-1) which colors dead cells and can be seen as red on 568 nm wavelength. The used stocks concentrations are 2 mM for EtHD-1 and 1 mM for Calcein AM. In this study 10 µl of EtHD-1 and 4 µl of Calcein AM were added into 20 ml of EB-Medium. The staining was done by removing the culture medium and then adding 500 µl of staining solution and incubating for 30 min in room temperature. The imaging was done immediately after staining using Olympus BX61W1 microscope with Hamamatsu ORCA-ER model C4742-80-12AG camera and cellM software.

3.5.2 Immunofluorescence

Double-Fluorescence protocol was used to stain the hiPSC-CMs cultures on textile structures. The staining was done in two parts. On the first day the samples were fixed, blocked and left in primary antibody solution overnight. The primary antibodies used were goat Troponin T (ab64623, Abcam) with dilution of 1:2000 and mouse Myosin binding protein C, MyBPC (sc-166081, Santa Cruz) with dilution of 1:400. On the second day the samples were exposed to secondary antibodies and then mounted on glass slips. The secondary antibodies used were Alexafluor 568 donkey anti-goat (Life Technologies) with dilution of 1:800 and Alexafluor 488 donkey anti-mouse (Life Technologies) with dilution of 1:800. The staining was done according to Figure 5 and the solutions and their reagents can be found in Table 5.

The stained samples were imaged with a Zeiss Imager.M2 Axio fluorescence microscope with ApoTome attachment and AxioCam MRm camera. Images were taken with both 10x and 40x objectives. Immunofluorescence images of hiPSC-CMs grown on textiles were compared to hiPSC-CMs grown on glass slips in the same circumstances, to see if the orientation of sarcomeres was higher in textile grown hiPSC-CM.

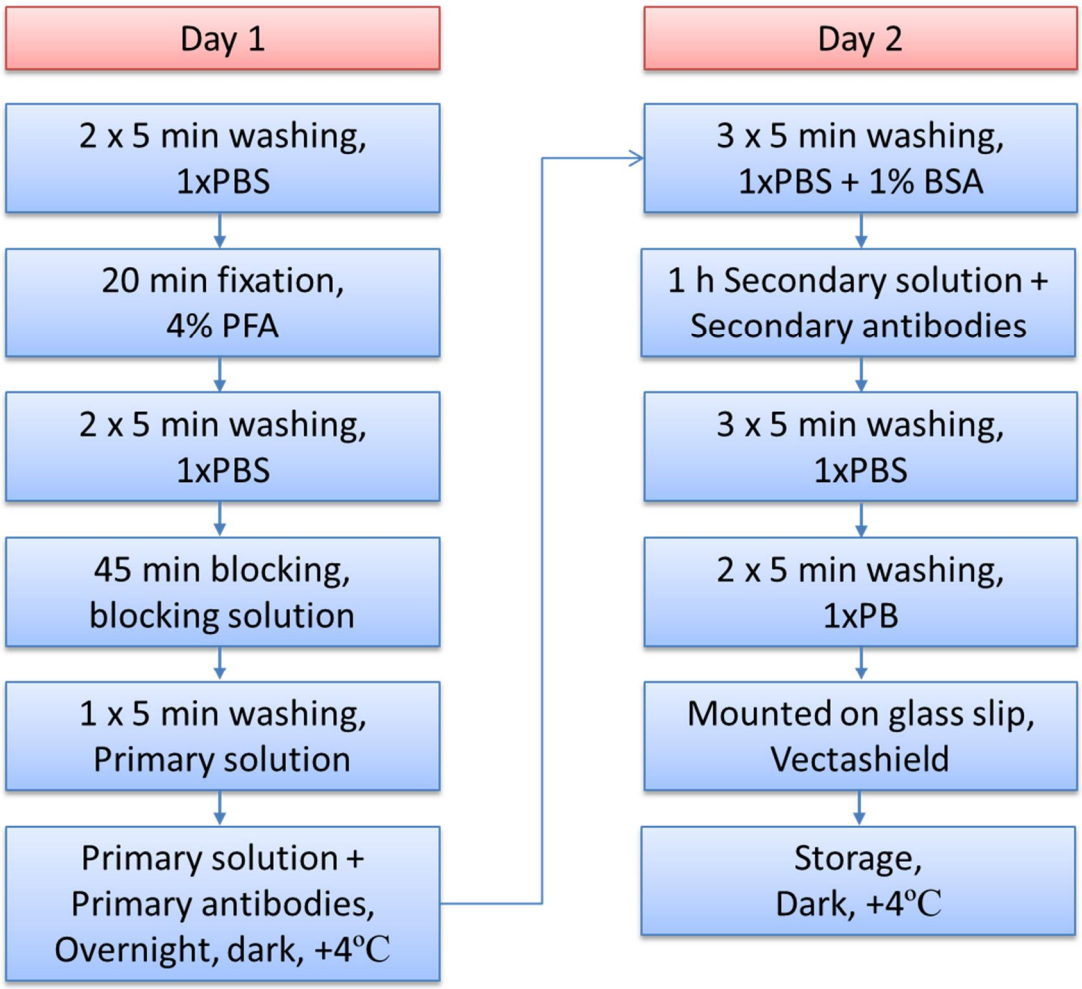

Figure 5. *Double-fluorescence staining protocol.*

Table 5. *Solutions used in immunofluorescence staining and their composition, PBS is phosphate buffered saline, BSA is bovine serum albumin, PB is phosphate buffer, NDS is normal donkey serum, DAPI is 4',6-Diamidine-2'-phenylindole dihydrochloride.*

Solution	**Reagents**
Washing solutions	1xPBS (Life Technologies)
	1xPBS 1% BSA (Sigma-Aldrich)
	1 x PB (Life Technologies)
Primary solution	1xPBS 1% NDS (Merck Millipore) 0.1% TritonX-100 (Sigma-Aldrich) 1% BSA
Fixation solution	4% PFA (Sigma-Aldrich)
Blocking solution	10% NDS 0.1% TritonX-100 1% BSA
Secondary solution	1xPBS 1% BSA
Mounting solution	Vectashield with DAPI (H-1200, Vector Lab)

3.5.3 Bright field

Bright field images and video were taken for two reasons. Firstly, the samples were checked to see whether the cells had attached or not, and secondly to see if any of the cells were spontaneously beating. Most of the bright field imaging was done on the control coverslips to see if the dissociation was successful. Bright field microscopy could not be used to detect cells on PETs. Something was seen on PLDLA textiles, but without staining it was not certain if they were heart cells or something else, like the coating material.

3.6 Analysis

The results of this study were mostly analyzed through imaging. The orientation was evaluated by using software called Cytospectre. CellProfiler was used to get an estimate of number of cells on each sample. Calcium imaging was primarily tested to see whether it could be done as it is one of the methods used at our group to study the effects of drugs on arrhythmia patient's cells. All the images were processed with ImageJ software before further analysis with Cytospectre and CellProfiler.

3.6.1 Cytospectre

The orientation of the cardiac cells was studied by using software called Cytospectre (Kartasalo et al. 2015). Cytospectre uses Fourier transform to estimate the power spectrum of the image taken from the cell. Based on the spectrum it calculates values that represent the orientation and the size of the cell structures. In this study the most important parameters were circular variance and detailed component's wavelength. Circular variance describes on scale from 0 to 1 how oriented the cell structures are. The value 0 would mean that every part of the cell structure is oriented in the same way i.e. in a line and 1 would mean that the structure orientation is equally distributed to all directions i.e. a circle. In short, the smaller the value of circular variance is, the higher the level of orientation is. Detailed component's wavelength values tell us the range of length in which the small structural parts, in this case sarcomeres, are. Cytospectre also determines the longest axis the cell spans over and the widest part perpendicular to the longitudinal axis. The relation of these values was used to determine whether the cells are more rod like or equally spread. (Kartasalo et al. 2015)

These properties were used to determine if the coated textiles offered increased orientation compared to cells grown on glass cover slips. It was also used to see if there were any differences between different coating materials and different textiles.

The cells that were analyzed with Cytospectre were chosen to be the ones with identifiable sarcomere structures. The images were segmented so that the Cytospectre analyzed only one cell at the time, not all the cells in the image. This caused there to be a difference in sample sizes as different images had different number of cells.

3.6.2 CellProfiler

The proportional number of cells on each sample was determined by using free software called CellProfiler. CellProfiler was used to calculate the number of nuclei in each immunostained 10x magnification image of the sample. 5 to 6 images were taken from each sample and the average nuclei count was determined. This value is used as a comparison number between samples and does not include all the cells in the sample. CellProfiler detects nuclei through several parameters, like size and shape. There was also a cutoff threshold for low levels of light intensity to remove false positive results. As the cell sizes, counts and shapes varied between and within samples, no other parameters than nuclei detection were used to determine cell counts. The number of cells plated in each experiment varied so the differences between the experiments are meaningless.

3.6.3 Calcium imaging

Calcium imaging was tested to if the calcium movement could be detected in the cell of if the fibers blocked the visibility. The calcium imaging was done by Risto-Pekka Pölönen from BioMediTech's Heart group.

3.6.4 Statistical analysis

Statistical analysis was done with IBM SPSS statistics 23 program. Because there were more than 2 groups compared to each other, T-test could not be used. The analysis was made with ANOVA-method (analysis of variance) using Bonferroni-correction to compensate the number of groups. This means that the limit of relevance was $p < 0.005/n$, where n is the number of groups in the analysis (McDonald 2014).

The statistical analysis was made in phase 2 for circular variance and sarcomere length. The analysis was done to see, if there was statistically relevant difference between different textiles and coatings. The difference in coatings was determined within each used textile type. To determine the difference between each textile, results for all coatings for the same textile were compiled as one. The compiled results for each textile were compared to each other to see if there were differences.

3.7 Experiment structure

The current study was done in two phases. The first phase was to determine which coatings would be used in the second phase. It was done to bring the sample sizes into more manageable level. The analysis was done by visually comparing the live/dead and immunostaining images between samples. In the second phase the cell amounts and cell structures were computationally analyzed from the immunostaining images. With the elimination of coatings in the first phase, the sample sizes and cell counts in the second phase were higher. This reduced the possible random deviation in the numerical values and made the results more reliable.

The basic structure of the tests was to coat the textiles with chosen materials, plate the cells on the coated samples and then test them at two time points. The workflow is presented in Figure 6. The textiles were washed with 70% ethanol and dried before coating to remove any contaminants. The textiles were then coated and the cells were plated on them. In the first phase, the two time points were used to determine if the cells attached properly (first time point) and if they detached over time (second time point). At first time point 1 textile and 1 control sample of each coating was tested. The first time point was after 4-5 days of the plating of cells. The rest of the samples were left to incubate for additional 3-6 days.

The second phase used only one time point. The chosen time point was after four days of incubation. This was chosen to remove the need of changing medium, which could also remove some of the detached and unattached cells. The growth wells, where the samples were incubated, were live/dead imaged. It was done to determine if just dead cells fall to the bottom or if living cells also pass through the samples. The cell amounts and the structural maturity were evaluated using CellProfiler and Cytospectre. In the last part of the second phase different textiles than the standard PET were used.

The different materials, analysis methods, cell lines and time points in different phases and experiments are shown in Table 6.

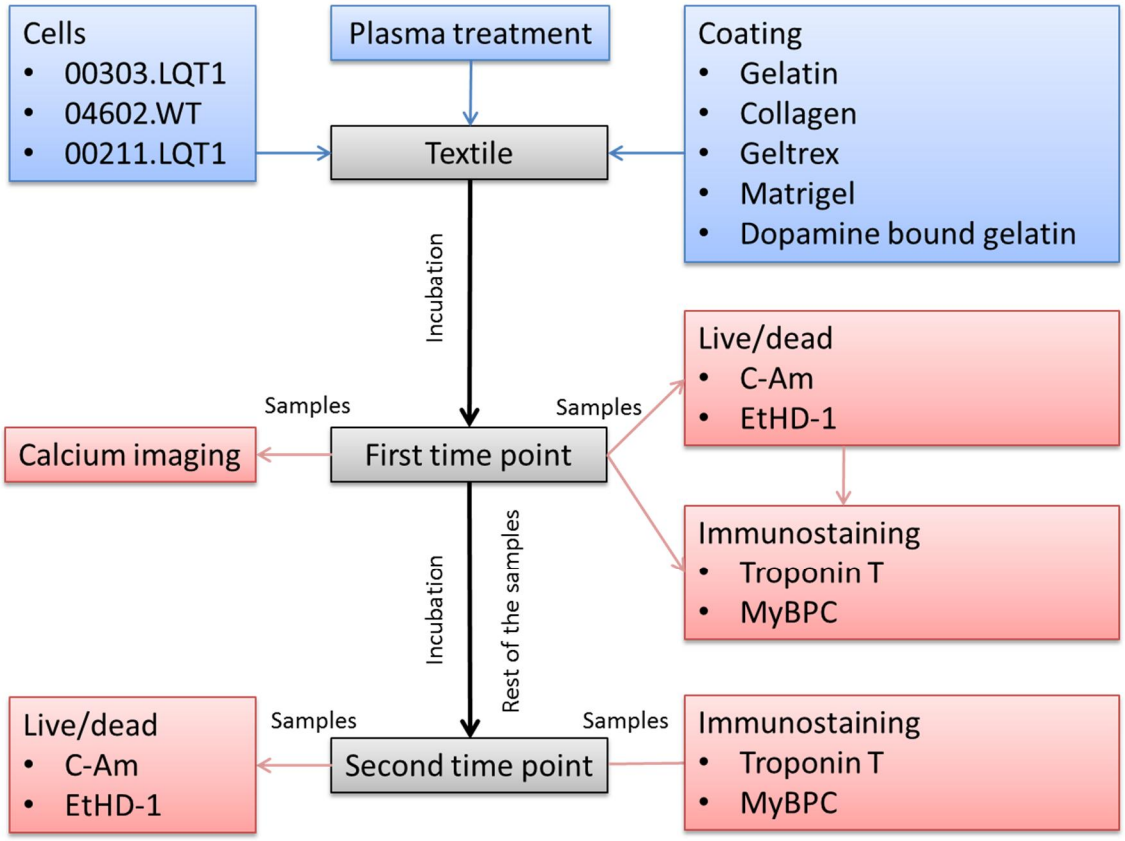

Figure 6. *The workflow. Each textile is first coated and the cells are then plated on it. The cells are left to incubate on the textile until the first time point where samples are taken to staining and imaging. The rest of the samples are left to incubate until the second time point where they are then taken to staining and imaging.*

Table 6. *The contents of the trials in both phases of the study. Time points are determined by considering that the cells are plaited on day 1.*

Phase	Trial	Textile	Coatings	Tests	Cells	Time Points
Phase 1	1	PET	Collagen Gelatin	Brightfield microscopy	00303.LQT1 ~1 beating area	Day 5 Day 11
	2	PET	Gelatin Geltrex Matrigel Collagen	Live/dead Immuno	04602.WT ~1 beating area	Day 5 Day 11
	3	PET	Gelatin Geltrex Matrigel Collagen	Calcium imaging	04602.WT ~1 beating area	Day 6
	4	PET	Gelatin Geltrex Matrigel	Live/dead Immuno	00211.LQT1 ~5 beating areas	Day 6 Day 9
	5	PET	Gelatin Dopamine bound gelatin Geltrex	Live/dead Immuno	00211.LQT1 ~2.5 beating areas	Day 5 Day 10
Phase 2	1	PET	Gelatin Dopamine bound gelatin Geltrex Plasma + gelatin Plasma	Live/dead (wells) Immuno	00211.LQT1 ~7 beating areas	Day 5
	2	PET	Plasma + Gelatin	Live/dead (wells) Immuno	00211.LQT1 ~5 beating areas	Day 5
		PLDLA	Gelatin Geltrex Plasma + Gelatin	Live/dead (wells) Immuno	00211.LQT1 ~5 beating areas	Day 5
		Derivate PET	Gelatin Geltrex Plasma + Gelatin	Live/dead (wells) Immuno	00211.LQT1 ~5 beating areas	Day 5

4. RESULTS

4.1 Coating optimization

In the first phase the PET textiles were coated with 5 different materials. This was done to determine which coatings would be used in phase two. The analysis of differences was made visually from live/dead- and immunostainings through microscopy.

Gelatin coating was considered the baseline and all the other coatings were compared to it. The other tested coating materials were collagen, Matrigel, Geltrex and dopamine bound gelatin.

4.1.1 Cell attachment

The number of cells found in live/dead and immunofluorescence imaging varied between the coating materials. The live/dead staining found only living C-AM stained cells (green) on the samples. There was no clear EtHD-1 staining of dead cells (red). There was some EtHD-1 staining but the shape was completely different from living cells. The EtHD-1 stained parts were small and particle like. They were also several times smaller than the living cells stained with C-AM. The EtHD-1 stained parts were determined to most likely be residual EtHD-1 or cell debris instead of dead cells.

Collagen coated samples had either fewer or same number of cells as gelatin coated samples. It was determined that collagen does not provide any improvement over gelatin.

Compared to gelatin, Geltrex and Matrigel coatings increased the number of cells found on samples. The number of cells found on Geltrex and Matrigel was similar and no clear difference between the two coatings could be determined.

Samples coated with dopamine bound gelatin had more attached cells than gelatin coated samples. There was also another difference. The cells on dopamine bound gelatin were clumped in small areas, whereas on the other coatings the cells had spread more evenly across the textile. Dopamine bound gelatin coatings also had some residual material left in the structure which was not found on any of the other coatings. It was most likely residual dopamine and it did not seem to have any effect on cell attachment.

4.1.2 Structural maturation of the cells

The samples were immunostained with Troponin T and MyBPC to determine the structure of cell. The MyBPC-stainings failed in phase one and the resulting images were blurry. The Troponin T staining was successful and it was used to determine the alignment

and structure of the cells. At phase one the structures were observed visually to determine whether they are more aligned or not.

There was no improvement in alignment on collagen coated samples compared to gelatin coatings. Matrigel and Geltrex coated samples were similar to each other and they provided the same or a bit greater level of alignment than gelatin coating. The difference was so small that it could not be verified without computational analysis.

Dopamine bound gelatin had two kinds of results. The clumped cells were round and were not as well aligned as on gelatin coatings. However, the non-clumped cells and the cells at the edges of the clumps were aligned similar to gelatin coated samples.

In all samples the cells grew longitudinally in relation to the fibers they were grown on.

4.1.3 Usability of analysis methods

All the samples could be imaged with live/dead staining and immunofluorescence. No dead cells were detected on the samples in live/dead assay. The MyBPC-staining was blurry and no clear structures could be detected.

All the coatings except dopamine bound gelatin were tested with calcium imaging. The cells and the flow of calcium could be detected on the samples.

4.2 Computational analysis

In phase two the goal was to produce numerical data values on the attachment and structural maturation of cells on differently coated textiles. The samples were immunofluorescence imaged and the images were computationally analyzed. The coating materials were chosen from phase one. Collagen did not provide any improvement over gelatin and it was left out from the rest of the experiments. Matrigel was removed from the rest of the experiments as there was no noticeable difference between Matrigel and Geltrex in any category. Geltrex was chosen over Matrigel as it is currently more used by the group in other applications. Dopamine was kept in the experiments, because it had been used in only one test, and one test was not enough to determine if it had positive effects on cell culturing. In addition, plasma treatment was used on phase two on part of the samples. Two completely new textiles were introduced in the last experiment of phase two. The textiles were blue plain woven derivate PET, and PLDLA-starfiber. The second phase used higher amounts of cells than phase one to increase the sample sizes.

4.2.1 Cell attachment

The attachment of cells was measured in two different ways. All the samples were stained with Troponin T, MyBPC and DAPI. The cell counts on each sample type were

determined by calculating the average number of DAPI stained nuclei on 10x magnification images. In the first experiment the average was calculated from 10 images (5 from each parallel sample). However, the actual sample size was smaller, as some of the images were poor quality and the CellProfiler software could not separate the nuclei from the autofluorescence of the fibers.

The other method was to image the growth wells, where the samples incubated, with live/dead colors to see if there were any living or dead cells that have detached or have not attached onto the samples.

The live/dead staining found that there was a large amount of both living and dead cells at the bottom of the growth wells. Parts of the wells were almost confluent. A large portion of the cells was observed to grow beneath the textiles with clear lines where the edge of the textile ends. Three surface treatments had higher amounts of cells at the edges of the well. The treatments were gelatin coating with or without plasma treatment and plasma treatment without coating. Other treatments had more cells beneath the textiles and less at the edges of the well.

All the sample textiles had living cells growing on them. There were differences between the coatings on the spreading of the cells. The gelatin coated, gelatin coated with plasma treatment and only plasma treated textiles had the most evenly spread cell populations and Geltrex had a little more concentration in the middle. Dopamine bound gelatin coated textiles on the other hand had very concentrated cell population in the middle, roughly on the spot where the cell suspension was applied, and the edges of the textile were almost completely void of cells. 10x magnification images of the samples with different coatings used in first experiment of phase 2 can be seen in Figure 7. Figure 8 has 10x magnification images of PET textile and control samples of second experiment in phase two. Figures 9 and 10 have similar images of plain woven derivate PET and PLDLA textiles from the second experiment of phase two.

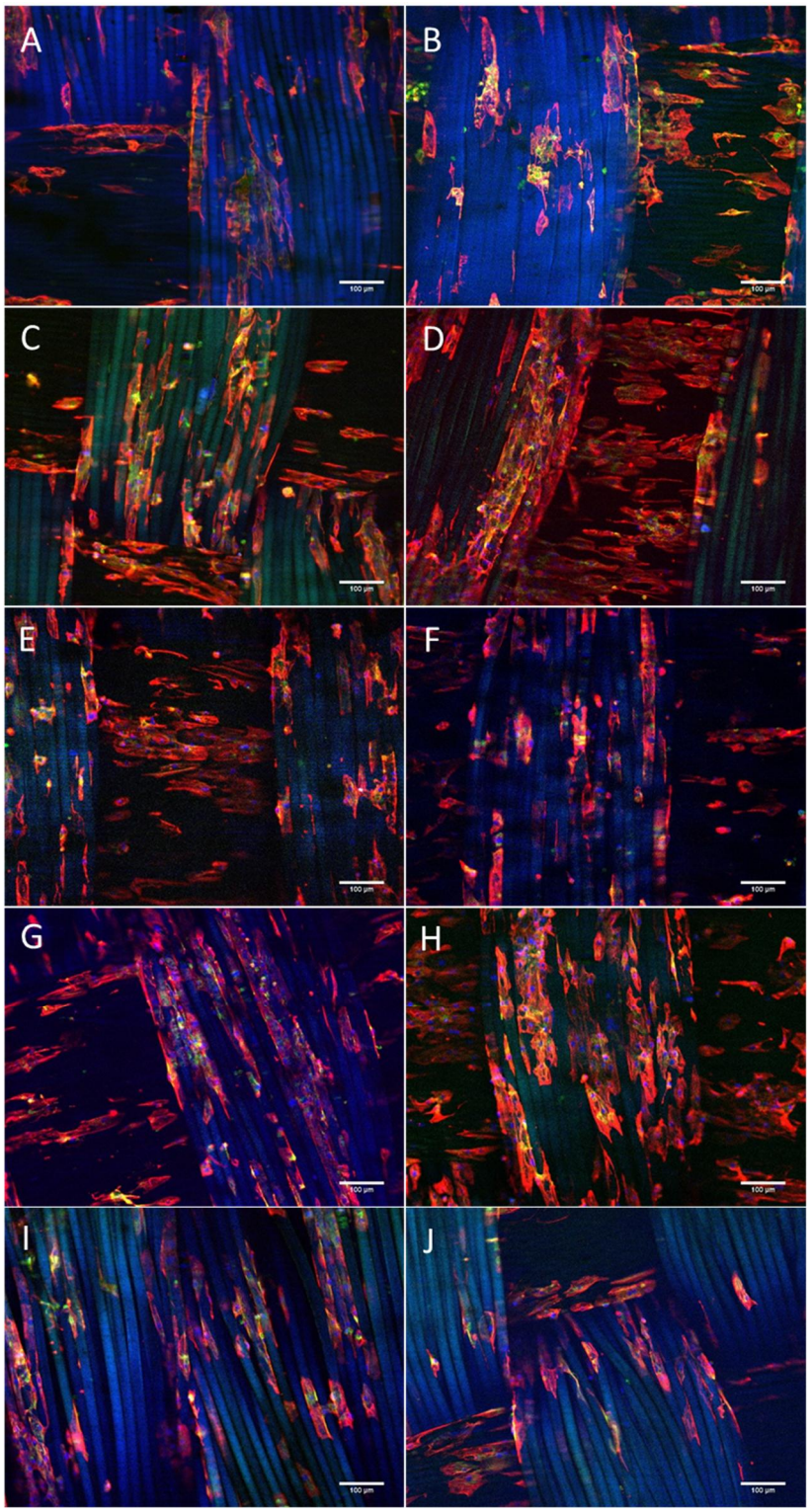

Figure 7. *Immunostained 10x magnification images of PET textiles from the first experiment. The blue color is DAPI, green is MyBPC, and red is Troponin T. There are 5 different surface treatments. A&B) are dopamine bound gelatin coated, C&D) are gelatin coated, E&F) are Geltrex coated, G&H) are plasma treated, I&J) are plasma treated and gelatin coated. There was blue autofluorescence from the fibers that was not DAPI. This is most notable in A&B. The scale bar is 100 µm.*

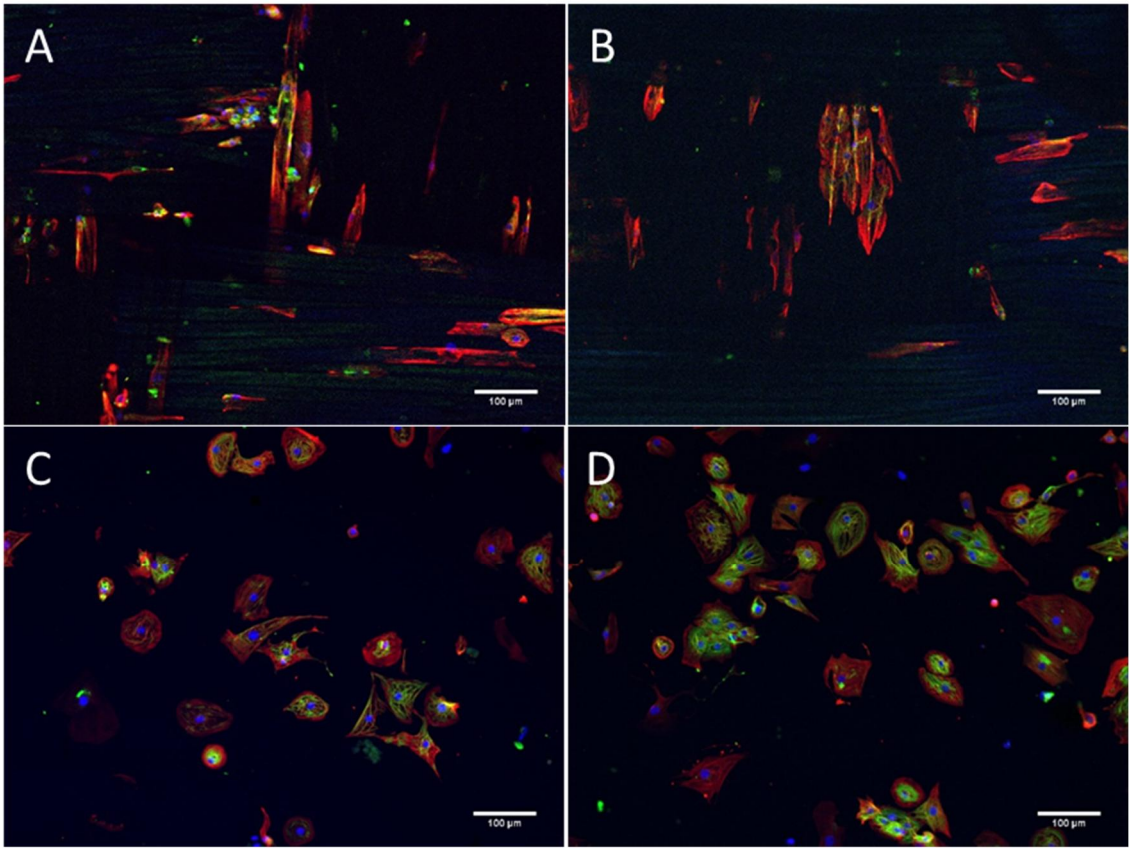

Figure 8. *Immunostained 10x magnification images of PET textiles and coverslips used as control samples from the second experiment. The blue color is DAPI, green is MyBPC, and red is Troponin T. A&B) are plasma treated and gelatin coated PET and C&D) are gelatin coated coverslips. The scale bar is 100 µm.*

The cell counts on each sample type were determined by calculating the average number of nuclei on 10x magnification images. In the first experiment the average was calculated from 10 images (5 from each parallel sample). However, the actual sample size was smaller, as some of the images were poor in quality and the CellProfiler software could not separate the nuclei from the autofluorescence of the fibers. This was most apparent with dopamine bound gelatin which was stained blue and no nuclei counts could be determined (Figure 7 A-B). On other surface treated PETs the average was calculated from 5 to 8 most successfully processed images. In the second experiment the average was calculated from 12 images (6 from each parallel sample). Unlike the first experiment the stainings were more successful in the second experiment and most of the images could be successfully processed in CellProfiler.

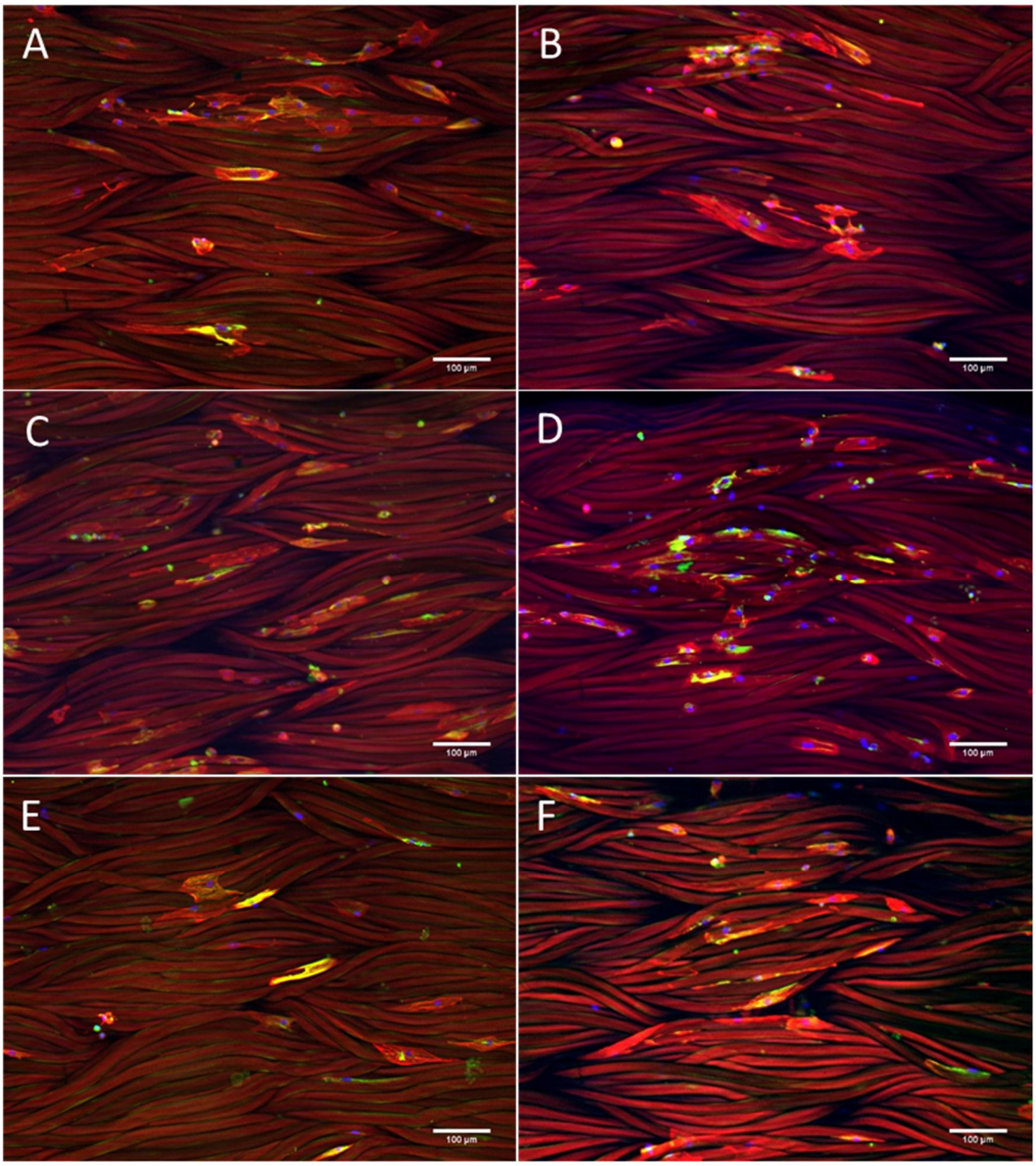

Figure 9. *Immunostained 10x magnification images of plain woven derivate PET textiles from the second experiment. The blue color is DAPI, green is MyBPC, and red is Troponin T. There are 3 different surface treatments. A&B) are gelatin coated, C&D) are Geltrex coated, E&F) are plasma treated and gelatin coated. There was red autofluorescence from the fibers that was not Troponin T. The scale bar is 100 µm.*

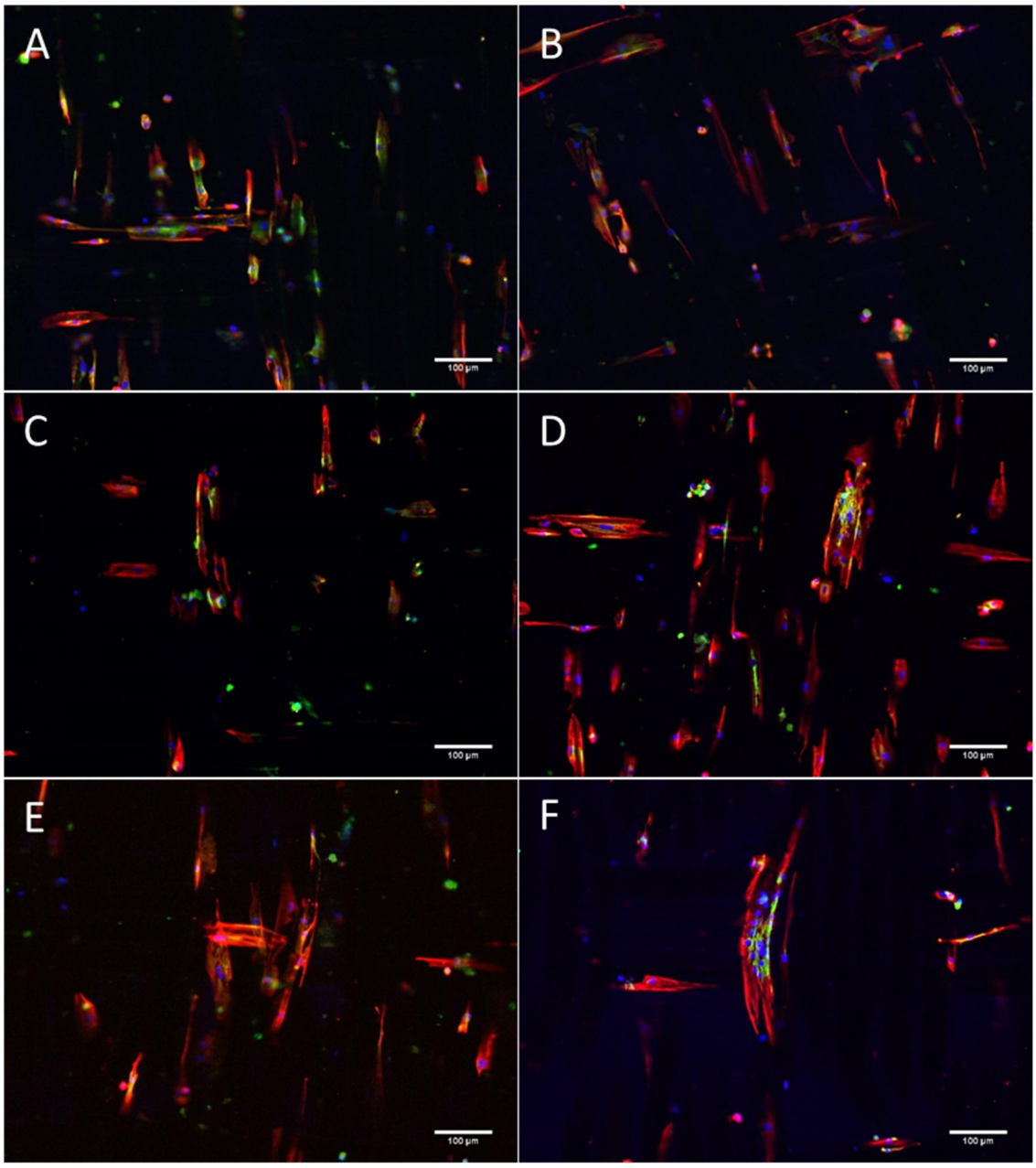

Figure 10. *Immunostained 10x magnification images of PLDLA starfiber textiles from the second experiment. The blue color is DAPI, green is MyBPC, and red is Troponin T. There are 3 different surface treatments. A&B) are gelatin coated, C&D) are Geltrex coated, E&F) are plasma treated and gelatin coated. The scale bar is 100 µm.*

In the first experiment, there were some differences between the number of cells found on the textiles. The number of cells in each imaged area varied a lot even within samples so the results on which coating material is the best are not clear. The average number of nuclei and the standard deviation between images in the first experiment are presented in Table 7 and Figure 11.

Table 7. *The average number of nuclei in 10 x magnification immunofluorescence images on different coating in the first experiment. Dopamine bound gelatin does not have values as the nuclei could not be detected, because of strong autofluorescence.*

Coating	Nuclei
Gelatin	155.7 ± 78.4
Geltrex	133.5 ± 51.7
Plasma	160.9 ± 80.6
Plasma gelatin	170 ± 35.5
Dopamine bound gelatin	-

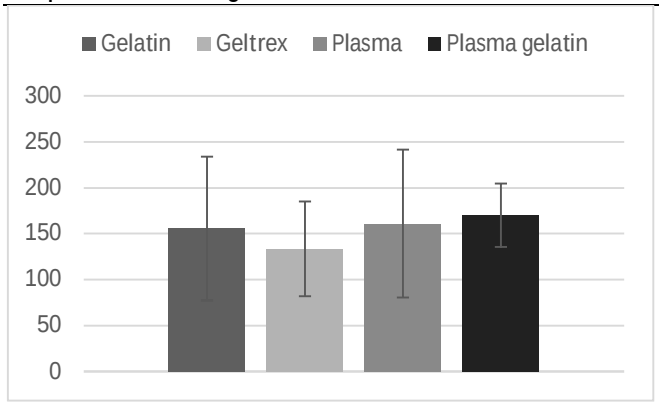

Figure 11. *The average number of nuclei and the standard deviation in 10 x magnification immunofluorescence images on different coating in the first experiment.*

There were fewer cells detected in the second experiment (Table 8) than in the first (Table 7), which was expected as there were less cells plated on the samples than in the first experiment. The most notable difference in nuclei counts was in plain woven derivate PET (Figure 12). The Geltrex coated samples had much higher average nuclei count on the textile (56.6 ± 24.5) than the other coatings (33.4 ± 18.2 and 38.2 ± 22.1). Surprisingly the nuclei count on plain woven derivate PET and PLDLA star-fiber were close to each other. It was expected that the transparent PLDLA would have more detectable nuclei than the plain woven derivate PET that was colored and only the layer on top of the fibers could be seen. The PET textile that was used in the previous experiments had the least number of nuclei.

Table 8. *The average number of nuclei 10 x magnification immunofluorescence images on differently treated textiles in the second experiment.*

	plain woven derivate PET	PLDLA	PET
Gelatin	33.4 ± 18.2	43.8 ± 12.9	
Geltrex	56.6 ± 24.5	46.4 ± 17.5	
Plasma gelatin	38.2 ± 22.1	34.9 ± 10.4	27.8 ± 18.3

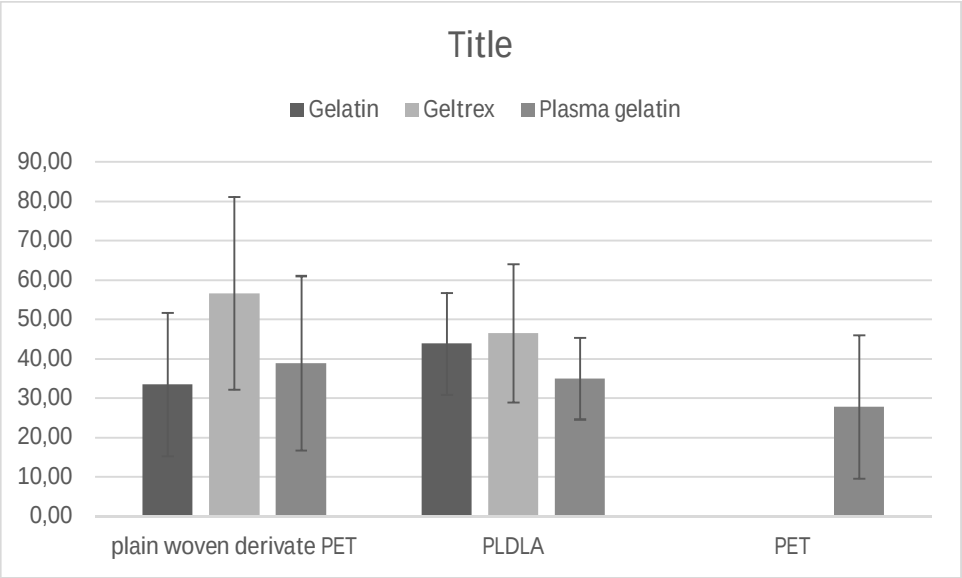

Figure 12. *The average number of nuclei in 10 x magnification immunofluorescence images on different coating in the second experiment.*

4.2.2 Structural maturation of the cells

The cell maturation was determined through the structural orientation of the cells. The structural properties of the cells were studied using immunostaining with 40x magnification. The images were processed with ImageJ and analyzed with Cytospectre after the fluorescence imaging. The prime properties on the structure and orientation of the cells were circular variance, modal wavelength of detail components and axis relations. Circular variance ranges from 0 to 1, zero meaning perfect alignment and 1 meaning no alignment. Modal wavelength tells the most common sarcomere length in the cell and axis relations tell the length to width proportions of the cell.

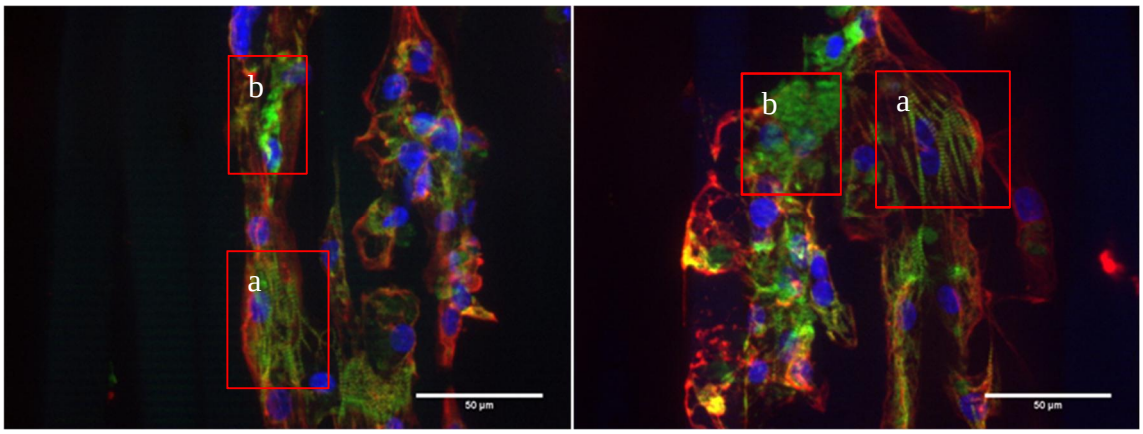

Figure 13. *40x magnification immunostaining images with both clearly visible sarcomere structures (a) and cloudy blurry colored areas without clear structures (b). The blue color is DAPI, green is MyBPC, and red is Troponin T. The scale bar is 50 µm.*

When imaging the cells in the first experiment the Troponin T and DAPI staining seemed good and clear but the MyBPC staining was blurry. The difference between clear sarcomere structure and blurry structure can be seen in Figure 13. Some of the cells have clear clean sarcomeres but many have only blurry green color with no clear structures. The images have been processed with ImageJ to reduce blurriness, but increased processing also affected the quality of clearly visible structures. Sample images for 40x magnification immunostaining images of Geltrex coated PET textiles and coverslips can be seen in Figure 14. Figure 15 has the same kind of images for gelatin coated, plasma treated and plasma treated with gelatin coating PETs and gelatin coated coverslips. Dopamine bound gelatin coated PETs and coverslips can be seen in Figure 16.

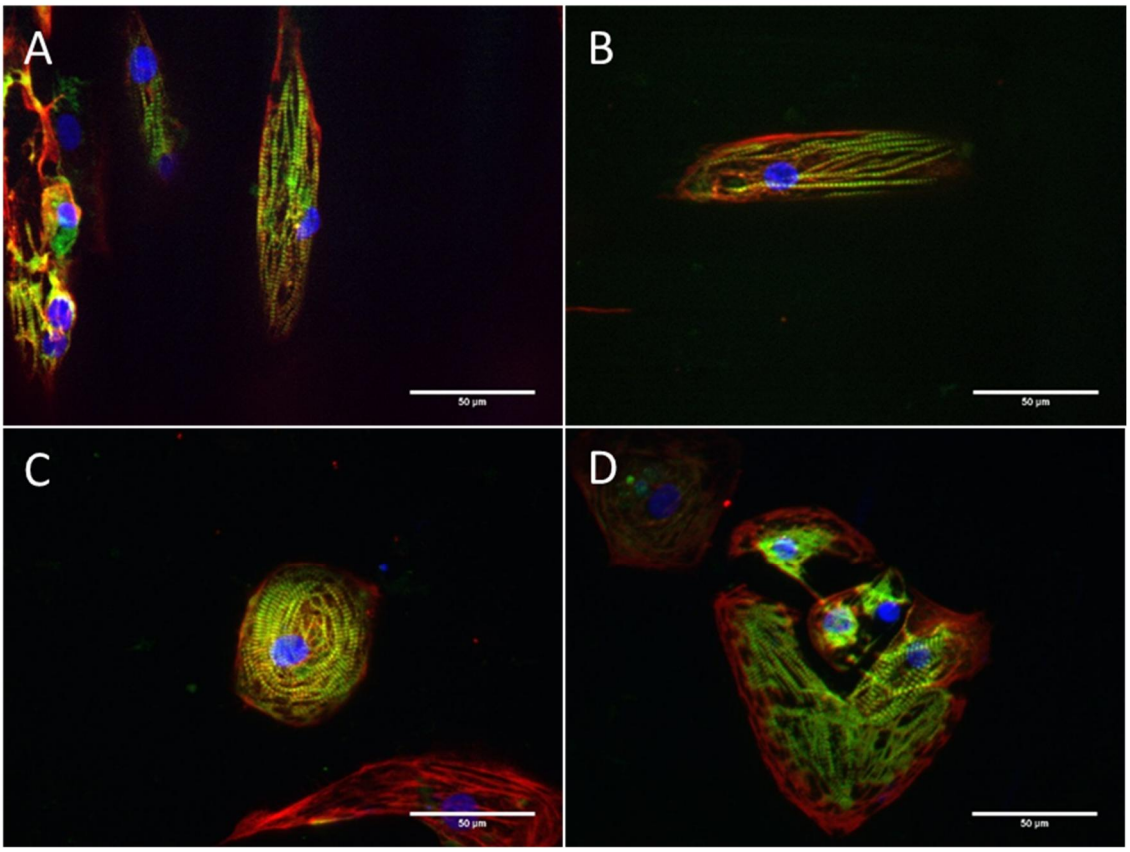

Figure 14. *Immunostained 40x magnification Images of Geltrex coated PET textiles (A&B) and coverslips (C&D) from first trial. The blue color is DAPI, green is MyBPC, and red is Troponin T. The scale bar is 50 µm.*

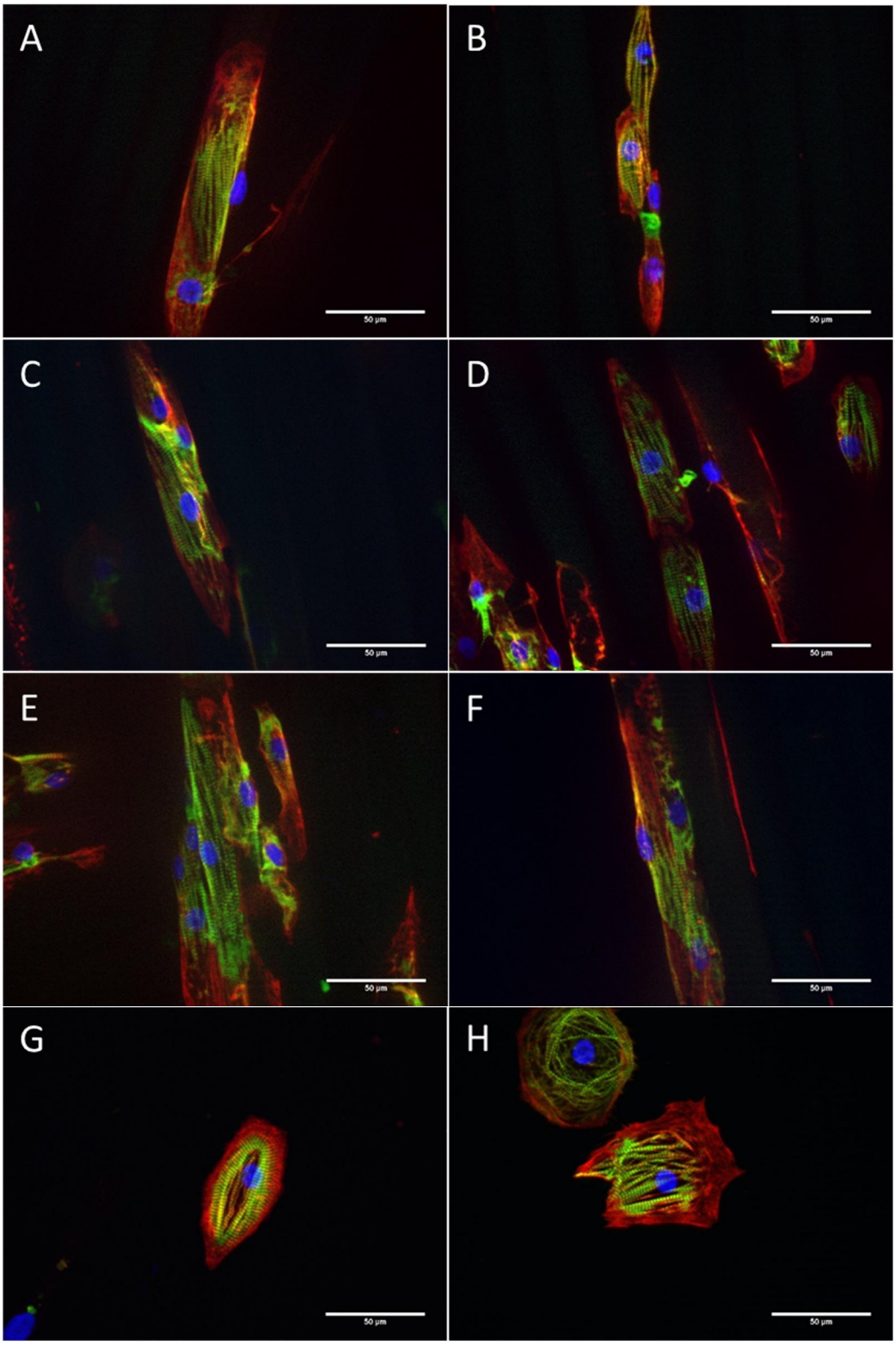

Figure 15. *Immunostained 40x magnification images of PET textiles (A-F) and control coverslips (G-H) from the first experiment. The blue color is DAPI, green is MyBPC, and red is Troponin T. There are 4 different surface treatments. (A&B) are gelatin coated, (C&D) are plasma treated, (E&F) are plasma treated and gelatin coated, (G&H) are gelatin coated coverslips. The scale bar is 50 µm.*

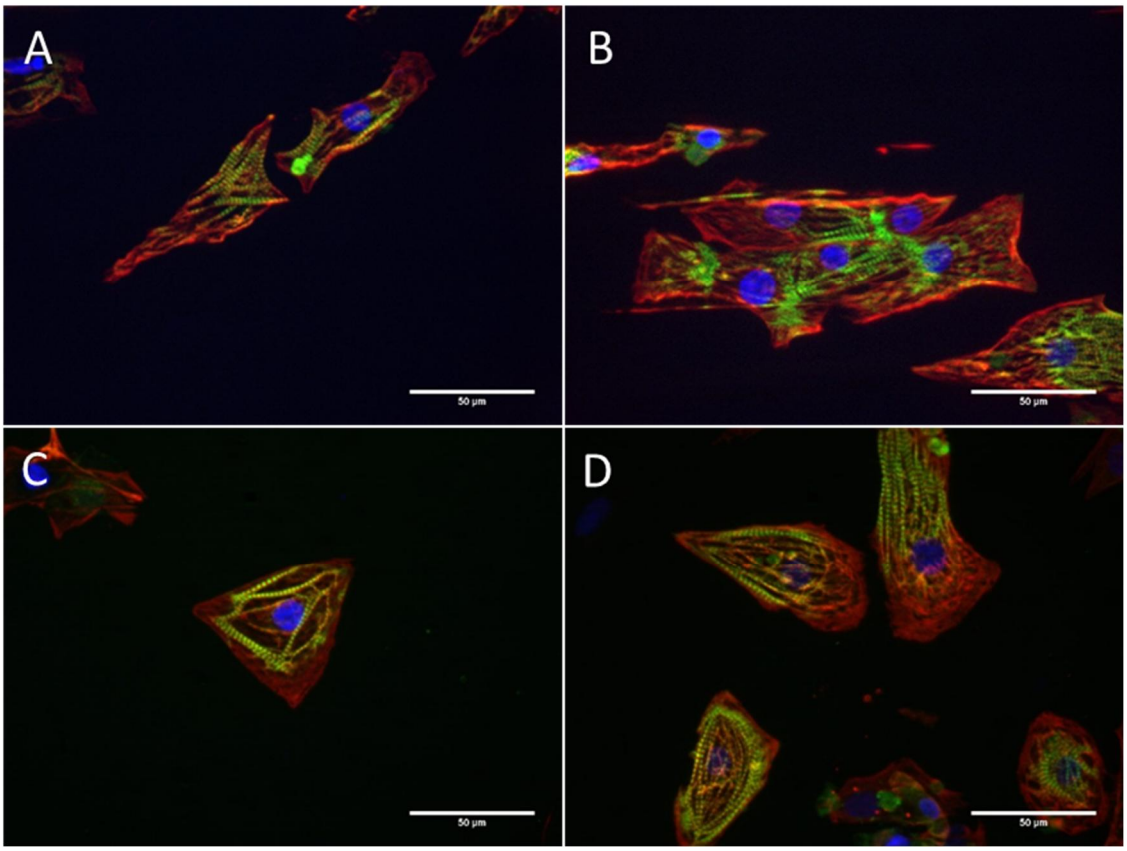

Figure 16. *Immunostained 40x magnification Images of Dopamine bound gelatin coated PET textiles (A&B) and coverslips (C&D) from first trial. The blue color is DAPI, green is MyBPC, and red is Troponin T. The scale bar is 50 µm.*

In the second experiment with PET, plain woven derivate PET and star-fiber PLDLA the immunostainings were better than in the first experiment. Examples for 40x magnification immunostaining images of plain woven derivate PETs can be seen in Figure 17, for PLDLA star-fiber in Figure 18 and for PET and control coverslips in Figure 19. The structures were clear and required less exposure time. There were still some cells that did not have clear sarcomere structures and they were blurry. The plain woven derivate PET with Geltrex coating had the highest number of cells with clear sarcomere structures.

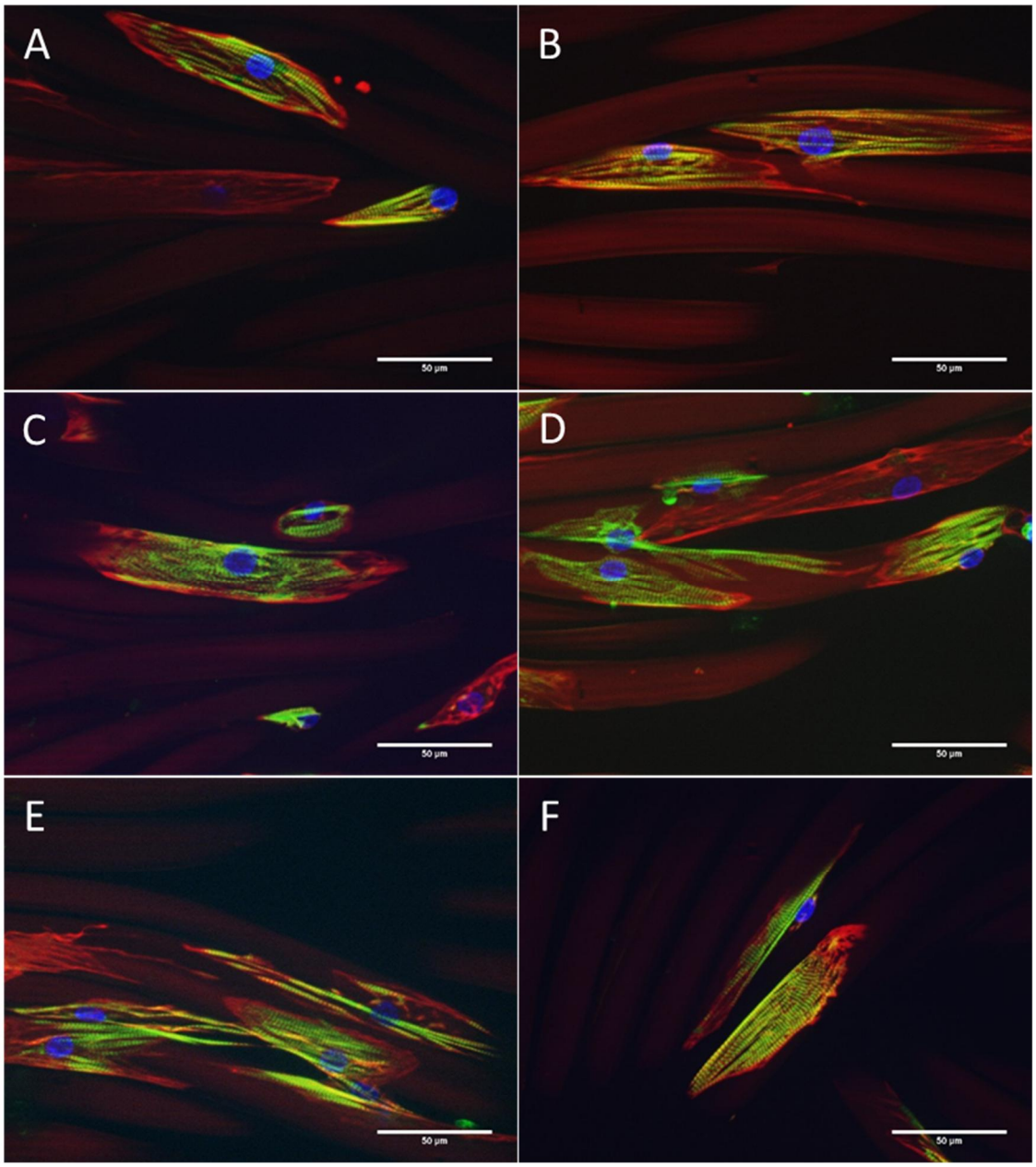

Figure 17. *Immunostained 40x magnification images of plain weave derivate PET textiles from the second experiment. The blue color is DAPI, green is MyBPC, and red is Troponin T. There are 3 different surface treatments. A&B) are gelatin coated, C&D) are Geltrex coated, E&F) are plasma treated and gelatin coated. There was red autofluorescence from the fibers that was not Troponin T. The scale bar is 50 µm.*

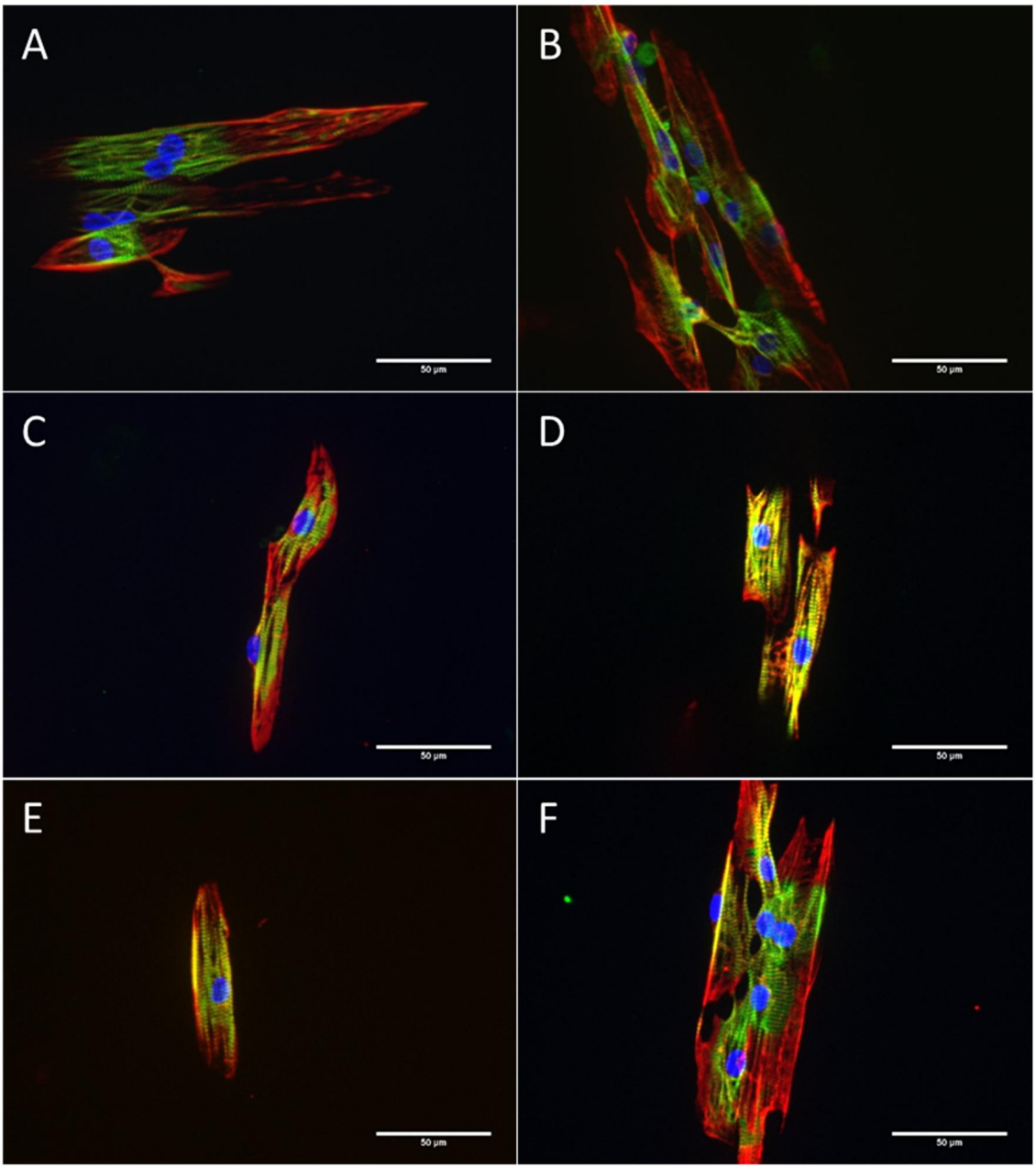

Figure 18. *Immunostained 40x magnification images PLDLA star-fiber textiles from the second experiment. The blue color is DAPI, green is MyBPC, and red is Troponin T. There are 3 different surface treatments. A&B) are gelatin coated, C&D) are Geltrex coated, E&F) are plasma treated and gelatin coated. The scale bar is 50 µm.*

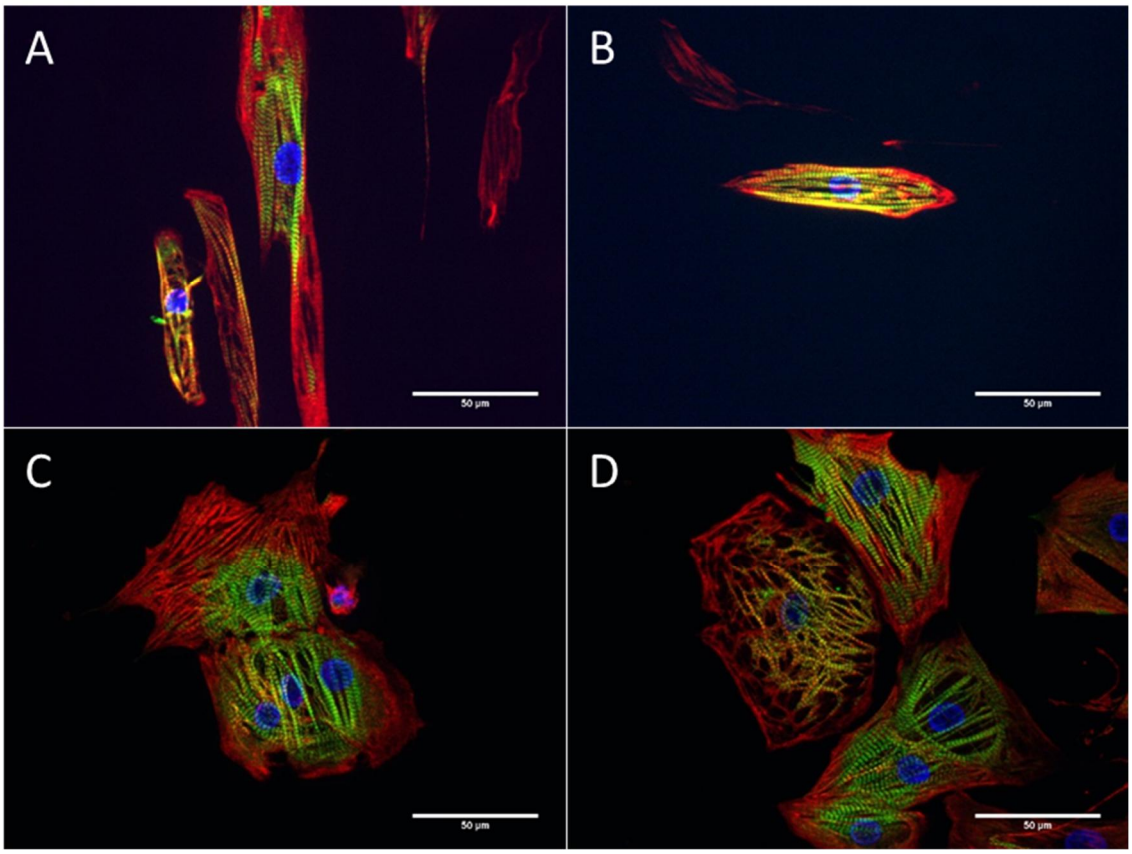

Figure 19. *Immunostained 40x magnification images of PET textiles (A-B) with plasma treatment and gelatin coating and control coverslips (C-D) with gelatin coating from the second experiment. The blue color is DAPI, green is MyBPC, and red is Troponin T. The scale bar is 50 µm.*

The cells that were analyzed with Cytospectre were chosen to be the ones with identifiable sarcomere structures (examples in Figures 14-19). The images were segmented so that the Cytospectre analyzed only one cell at the time. This caused there to be a difference in sample sizes as different images had a different amount of cell. The average values and standard deviations for all of the samples in phase two are in Table 9.

The average circular variances within each textile type were close to each other, but the results did vary between the textiles (Figure 20). The differences between the textiles and the controls were statistically significant ($p < 0.01$). The differences and statistical relevancies are presented in Figure 21. Within each textile, the differences between coatings were small (Figure 22). The plain woven derivate PET had the best results with average circular variances between 0.22 and 0.28 with standard deviations between 0.07 and 0.08. Both average circular variances and their standard deviations were smallest with average of 0.25 and 0.08 respectively. There were somewhat significant differences between the coatings. Both gelatin and plasma gelatin had lower average circular variance than Geltrex ($p < 0.05$). However, there was no significant difference between gelatin and plasma gelatin ($p = 1.000$). PLDLA and PET had larger average circular variances and standard deviations than plain woven derivate PET. PLDLA's average circular variances

were between 0.30 and 0.36 with average of 0.33 for all coatings and standard deviations between 0.15 and 0.18 with average of 0.16 for all coatings. There were no significant differences between the coatings ($p > 0.900$). The PET's average circular variances and their standard deviations were between 0.35-0.46 with average of 0.40 and 0.10-0.15 with average of 0.14, respectively. There was no significant difference between gelatin, Geltrex, dopamine bound gelatin and plasma gelatin ($p = 1.000$). The plasma treated PET without coating differed more. The significance values were between 0.088 and 1.000 (Figure 22). The control samples had average circular variances of over 0.6. The significance of the differences between the differently coated controls varied between $0.352 < p < 1.000$ (Figure 22).

The sarcomere lengths were similar to each other in all the textiles and coatings as can be seen in Figure 23. The differences between textiles were not statistically significant ($p = 1.000$) except for PLDLA (Figure 21). The only somewhat significant difference was between PET and PLDLA ($p < 0.05$). The differences between PLDLA and plain woven derivate PET and controls were not as significant ($p > 0.26$). Within each textile, the differences between coatings were small. The plain woven derivate PET and PLDLA had the smallest differences and there were no statistically significant differences between samples ($p = 1.000$) for either textile. The plain woven derivate PET's average modal length varied between 1.66 and 1.68 with average of 1.67 between all coatings and standard deviation varied between 0.06 and 0.13. For PLDLA the respective values were between 1.67 and 1.69 with average of 1.68 and standard deviation between 0.16 and 0.19. PET had similar average sarcomere length of 1.63 for all the coatings, even though the differences between samples were somewhat higher with values varying between 1.56 and 1.70 with standard deviations between 0.13 and 0.33. The statistical significance of the difference varied between $0.328 < p < 1.000$ (Figure 24).

The length width relation of textile is presented in Figure 25. Plain woven derivate PET had the highest average axis relations across all the coatings with the average value of 4.27 compared to PLDLA's 3.61 and PET's 3.37. Again, the standard deviations were large 1.70, 1.41 and 1.38 for plain woven derivate PET, PLDLA and PET respectively. The only clear difference was the control samples with only average axis relation of 1.7 across all coatings.

Table 9. *The average structural properties and standard deviations for all samples from the second phase.*

	Average circular variance (0-1)	Average modal sarcomere length (µm)	Average axis relations (length/width)	n (cells)*
PET				
Gelatin	0,363 ± 0,098	1,64 ± 0,25	3,71 ± 1,07	14
Geltrex	0,349 ± 0,139	1,56 ± 0,13	3,53 ± 1,27	22
Dopamin gelatin	0,422 ± 0,143	1,60 ± 0,33	2,90 ± 1,64	19
Plasma gelatin	0,387 ± 0,149	1,68 ± 0,16	3,74 ± 1,77	54**
Plasma	0,457 ± 0,147	1,70 ± 0,23	3,01 ± 1,16	30
PLDLA 96/4 Star-fiber				
Gelatin	0,305 ± 0,146	1,67 ± 0,19	4,20 ± 1,92	23
Plasma gelatin	0,355 ± 0,156	1,69 ± 0,19	3,26 ± 0,93	22
Geltrex	0,331 ± 0,183	1,67 ± 0,16	3,39 ± 1,39	21
Plain woven derivate PET				
Gelatin	0,228 ± 0,077	1,68 ± 0,13	4,69 ± 2,30	24
Plasma gelatin	0,223 ± 0,073	1,66 ± 0,06	4,22 ± 1,45	22
Geltrex	0,283 ± 0,080	1,66 ± 0,11	3,91 ± 1,36	25
Control				
Gelatin	0,697 ± 0,152	1,67 ± 0,11	1,53 ± 0,34	23**
Geltrex	0,714 ± 0,175	1,76 ± 0,22	1,79 ± 0,79	15
Dopamine gelatin	0,617 ± 0,202	1,87 ± 0,16	1,77 ± 0,55	19

* Number of cells depends on how many cells were segmented from each image

** Plasma gelatin PET and Gelatin controls were used in both experiments

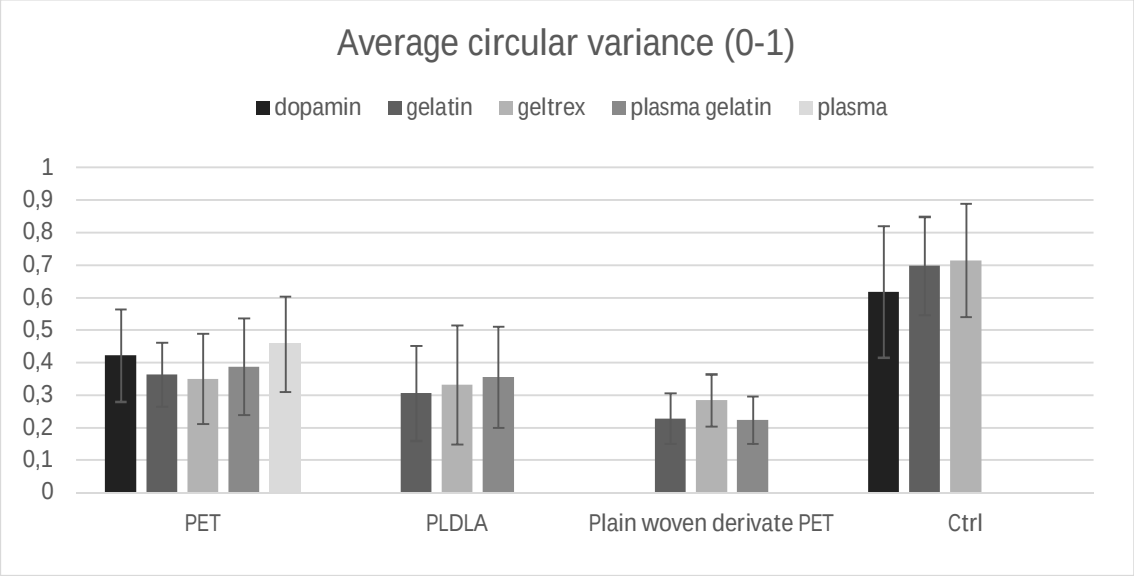

Figure 20. *The average circular variances and standard deviations for all the samples in phase two. All the textile types and each coating used are included.*

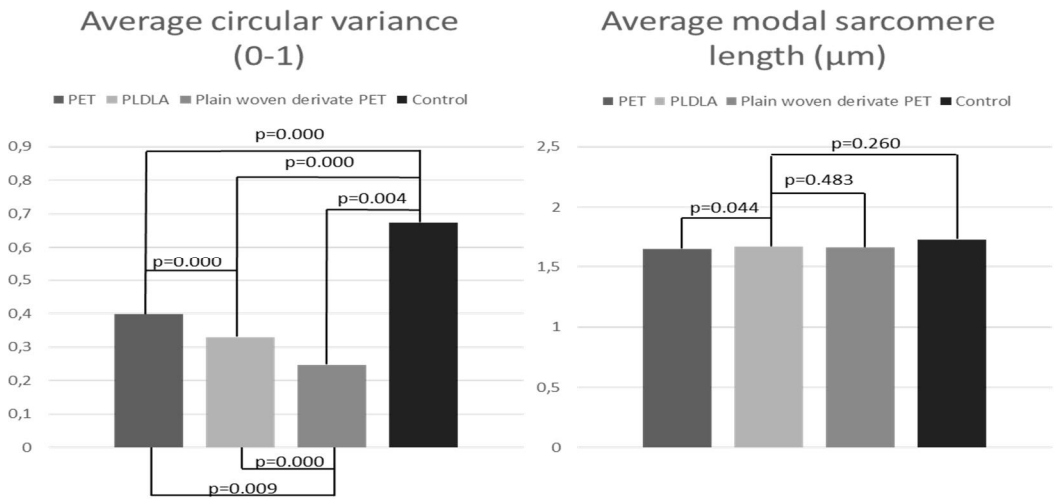

Figure 21. *Statistical relevance of differences in average circulars variance and modal sarcomere lengths of different textile samples. The averages include all coatings. Statistical relevance is given as p-value. The limit for statistical relevance is p < 0.0125 (Bonferroni correction). To keep the figures easy to read, p-values of 1.000 are not presented.*

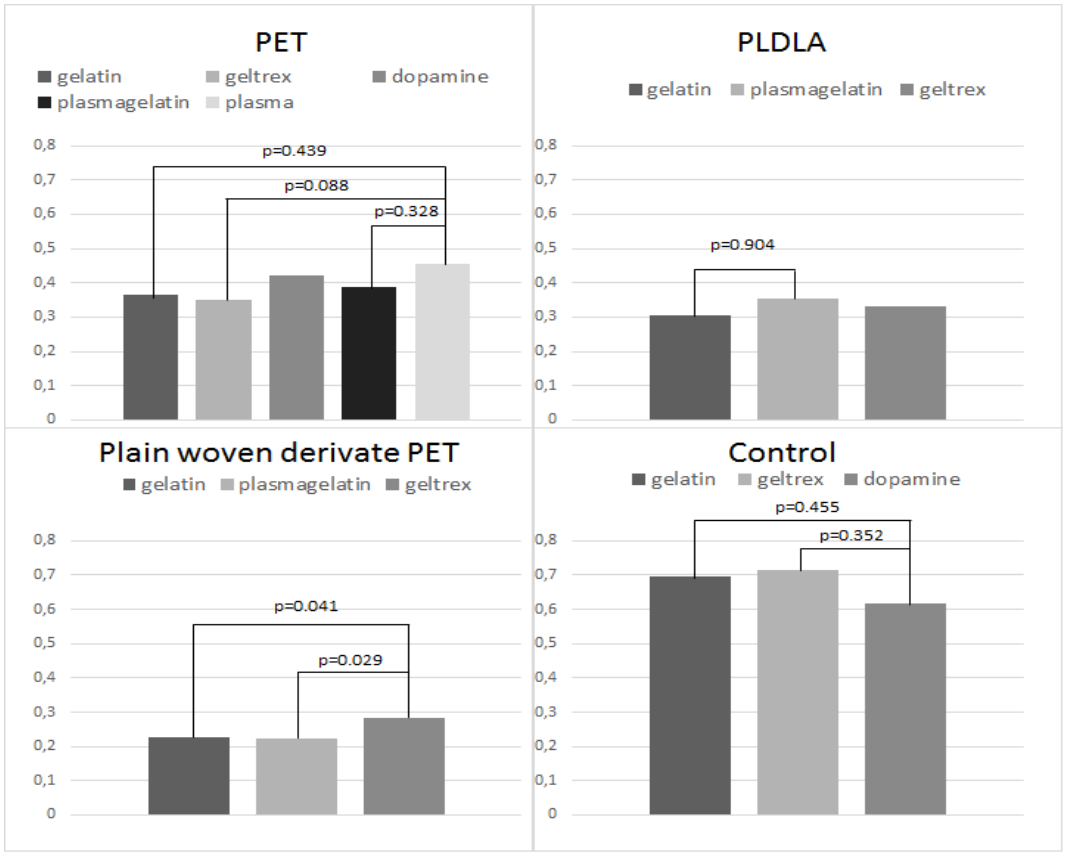

Figure 22. *Statistical relevance of differences in average circular variances (0-1) for each coating on each surface. Statistical relevance is given as p-value. The limit for statistical relevance is p < 0.01 for PET and p < 0.0167 for the rest (Bonferroni correction). To keep the figures easy to read, p-values of 1.000 are not presented.*

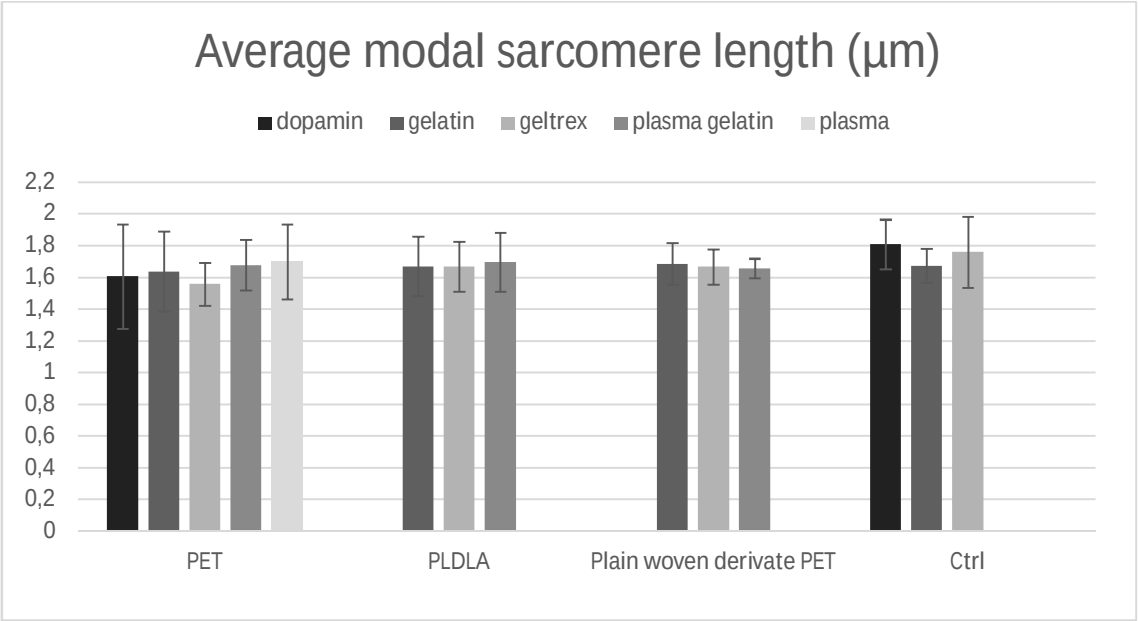

Figure 23. *The average modal sarcomere lengths and standard deviations for all the samples in phase two. All the textile types and each coating used are included.*

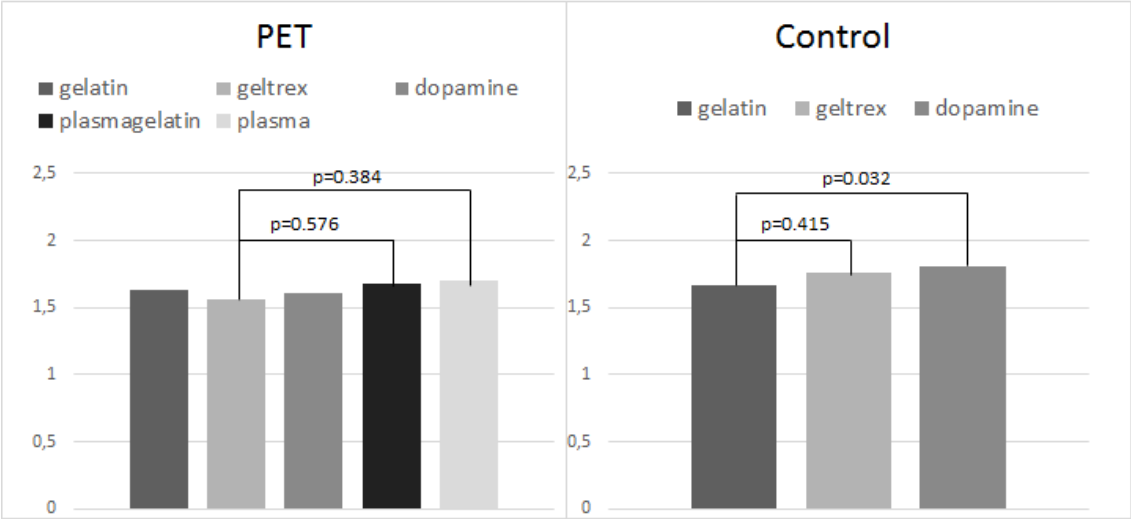

Figure 24. *Statistical relevance of differences in average modal sarcomere length for each coating. Statistical relevance is given as p-value. The limit for statistical relevance is $p < 0.01$ for PET and $p < 0.0167$ for controls (Bonferroni correction). To keep the figures easy to read, p-values of 1.000 are not presented (PLDLA and plain woven derivate PET only had p-values of 1.000).*

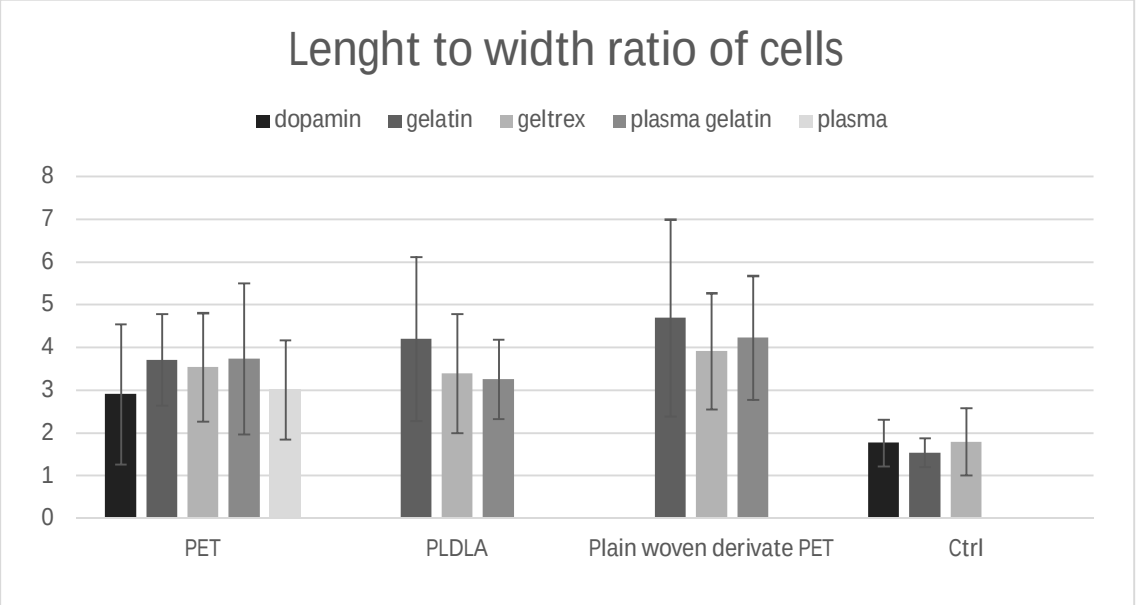

Figure 25. *The average length width relations standard deviations for all the samples in Phase two. All the textile types and each coating used are included.*

4.3 Other results

In the second phase, the analysis was done primarily from immunofluorescence images using CellProfiler and Cytospectre as analysis tools. There were some notable differences between different coatings and different textiles.

The 10x magnification images of PET textiles can be seen in Figure 7. The dopamine bound gelatin (Figure 7 A-B) emitted blue light on 10x magnification in fluorescence microscopy, making the detection and identifying of cell nuclei hard, as the nucleus is stained blue with DAPI. CellProfiler could not detect the nuclei reliably so the nuclei count for dopamine bound gelatin had to be left out from the results.

The blue plain weave derivate PET had strong autofluorescence allowing only the cells on top of the textile to be imaged as can be seen in Figures 9 and 17. The cells in between and under the fibers could not be seen or only be seen extremely faintly which caused then to be unanalyzable.

The PLDLA star-fiber (Figure 10 and 18) was the complete opposite as it was totally transparent and all the cells on all parts of the fiber could be seen. The cells could be clearly seen through the fibers which caused the fibers to refract the light making some of the images blurry. The PLDLA had another problem. The textile was thicker than the PET samples which made the cells grow more in 3D. This caused the image stacks to be twice as large causing increased blurriness in the images as the light from the lower parts of the cell interfered with the focus. The thickness had another negative result as the focusing in the lower parts of the textile became difficult. The objective of the microscope

came into direct contact with the cover glass and the wanted focus could not always be reached.

The PET textiles were not strongly colored so the cells could be detected more easily and they were not completely transparent which reduced the amount of refractions.

5. DISCUSSION

In a previous study (Junnila 2016) our group had determined that PET textiles could be used as growth surfaces and that they increase the orientation in cell structures. However, only a small number of cells could be detected on the textile. Three things were considered as the reason for the lack of found cells. The cells do not attach to the textile, they detach from the textile, and that the textile prevents the detection of the cells. In the current study the problem was approached in several ways. The amount of plated cells was increased, different coating materials were used to increase attachment, the samples were analyzed at two time points and the growth wells of the samples were analyzed to find what happened to the cells. The analysis of the samples was done through live/dead and immunofluorescence staining.

5.1 Cell attachment

The attachment of cells was studied through two methods. The number of cells attached to the textile was determined through calculating the amount of DAPI stained nuclei on each sample. The nuclei were calculated from the 5-6 10x magnification immunostained images with CellProfiler. The choice of using only nuclei to determine the cell amount was made so that one suitable workflow within CellProfiler could be done for all samples. The analysis of entire cells would have been hard as they varied on size, how clumped they were and how well the staining of different cell parts had succeeded. Using other variables would have made a standard detection method for cells extremely difficult to make. Nuclei themselves are similar in size and shape and quite clearly distinguishable from each other unlike other parts of the cell. The choice had some problems. Only nuclei were detected so CellProfiler determined that all nuclei belong to CMs, when there might have been other cells growing on the textiles. Another problem was that CMs can be multinucleated as well as mononucleated. This means that all the detected multinucleated CMs were calculated as different mononucleated cells. However, the relative amounts of cells between the samples in each trial should be comparable. This is because all the cells were from same cell suspension, so the amount of non-CMs and the ratio of mononucleated to multinucleated cells in each sample should be roughly the same. This is under the assumption that the coatings and textile materials and patterns did not affect the amount of attached non-CMs and that they did not promote multinucleation.

There were also other variables that increased the unreliability of the cell count. The images were taken manually without any systematic method, meaning that there is some bias towards highly populated areas and areas where the cells can be clearly seen. Although the method was the same for all of the samples this can easily cause error especially when the cells are not equally spread over the whole sample like with dopamine

bound gelatin samples. To get more unbiased result the samples should be imaged in some pattern that is the same for each sample and that has enough imaging points to reduce random differences within the results.

Another source of error was the accuracy of detection of the nuclei by CellProfiler. There were many false positives and false negatives. Some nuclei that were clearly visible in the image were not detected in CellProfiler. This was mostly due to the low intensity of light coming from the nuclei as there was a cut of limit that discarded all results with lower intensity than the threshold value. The cut of point was necessary to reduce the number of false positives. Even with the threshold and other image processing, the software detected false positives from the autofluorescence of the textiles. The false positive problem was bigger in some samples than others. The samples from the second experiment had fewer problems than in the first experiment. The worst case was dopamine bound gelatin PET. No results could be produced due to so high autofluorescence that no nuclei could be detected (Figure 7 A-B). Due to difference in the nuclei detection some of the images were left out from the results. In the first experiment, approximately half of the images were left out and all the dopamine bound gelatin images were discarded. This could affect the reliability of the results as some images had to be dropped and the remaining images might not represent the whole of the textile accurately. In the second trial only a few of the images had to be discarded due to clear errors. This difference was most likely due to the better success in the staining protocol as the images of the second experiment were clearer in general, compared to images of the first experiment. Taking these reasons into consideration, the cell count numbers are unreliable and cannot be used as absolute values. However, they do prove that cells can be grown on the textiles even in larger numbers. They can also be used to give a rough estimate of the relative differences between sample types within each experiment. Due to the uncertainty, the cell counts were not statistically analyzed.

There were some interesting results on the number of cells detected on the textiles. As the plain woven derivate PET was blue and had high autofluorescence and only the top most layer could be imaged, it was expected that it would have the lowest number of detected cells. Instead of this, all surface treatments had higher number of cells than the other PET and the Geltrex coated had more than the PLDLA textiles. The reason for this is not known, but it was suspected that the different textile pattern makes the gaps between the yarns smaller. The smaller gaps probably prevent most of the cells from passing through the textile which is most apparent in Geltrex which makes thicker coating that further prevents the cells from passing through. To find the exact reason for this result, each material should be tested with each weaving pattern to determine if the effect comes from the material or the pattern.

The other method to study attachment was to analyze the growth wells of the samples. This was done by removing the samples from the growth wells and staining the wells with

live/dead colors without changing the culture medium. This was done to prevent the loss of any live or dead cells in the medium. Both live and dead cells were found in the wells. The cells were primarily positioned under the textiles. Clear lines where the textile had been could be seen on where the cells were growing in the well. This suggests that when the cells are plated on the textile they initially stick to the coating material but slowly migrate through the textile and end up in the bottom of the well. To reduce the number of cells passing through, textile with smaller gaps between threads should be used. Other possibility is to user stronger coatings that do not let the cells go through them.

5.2 Structural maturation

The structural properties of the CMs were determined with CytoSpectre from 40x magnification immunofluorescence images. All the properties were calculated from the green channel of the images, which are the sarcomere structures stained with MyBPC. The properties that were determined were circular variance, modal wavelength of detail components and axis relations. The cells used in the structural orientation determination were chosen from the images with clearest sarcomere structures as the properties could not be determined if the images were unclear. This creates bias towards good results, which should be considered. The choosing process was the same for all samples so the relative values should be comparable. The culture times for the measured samples were short, only 4 days whereas in other studies the culturing times of 10+ days have been used (Rao et al. 2013, Han et al. 2016). Our previous study (Junnila 2016) had a 10-day culture time and it had better average orientation values. The choice was made to have faster results and to remove the need of medium change which would have affected attachment testing by possibly removing living and dead cells from the culture.

The average circular variances between different textiles had significant differences. When using ANOVA-method and Bonferroni correction the limit for statistical relevance for four different groups was $p < 0.0125$. The p-values between all textiles and controls were less than that, as can be seen in Figure 21. This means that the different growth surface significantly affected the average circular variance of sarcomere structures in hiPSC-CMs. The averages were calculated from all coatings. The sample amounts and the coatings used for each textile varied (Table 9), which could cause some of the differences between textiles. In the future, to make sure that the textile is the source of the difference, each textile should be compared to each other by using the same coatings and large enough sample sizes.

The plain woven derivate PET had the lowest average circular variances and the lowest standard deviations. This could be because only the top most layer of the textile could be imaged and only the cells on the top most layer could be seen. This means that all the detected cells had more similar growth surface compared to other textiles where the cells could grow in between the fibers and had more 3D oriented growth surface. To determine

the cause of the better circular variance each textile material should be tested with each weave pattern.

The differences between coatings within each textile were not as significant (Figure 22). There were no differences with significance of $p < 0.0125$. However, the differences between some coatings were close to that. The significance of the difference between Geltrex coated and plasma treated PET had p-value of 0.088. The Geltrex coated plain woven derivate PET had somewhat significant differences compared to gelatin coated ($p = 0.041$) and plasma treated, gelatin coated ($p = 0.029$) samples. Even though these values are not under the significance threshold ($p < 0.0125$), they might be somewhat significant as most of the p-values between coatings were 1.000.

The sarcomere lengths for all textiles and coating and even controls were between 1.56 µm and 1.87 µm. There were no statistically significant differences between textiles (Figure 21) or between coatings (Figure 24). If the result is compared to literature values (Mummery et al. 2012; Robertson et al. 2013; Yang et al. 2014) the length of the sarcomere is closer to that of immature CMs (1.6 µm) than mature (2.2 µm) CMs. However, this can be partly due to the short culturing time (4 days).

For the length width relations, all the textiles and coatings had clearly higher values than the control samples (Table 9). Differences between the coatings were small but textiles improved the elongation of the CMs compared to controls. There were some problems in the ratio determination. In some instances, the cells were easy to determine from each other (e.g. Figures 14 b, 15 d and 17 c) but in others it was hard (e.g. Figures 15 e, 17 e, 18 f). As the sarcomeres were most often in the same direction, the segmentation of the cells did not have a huge effect on the circular variance but it did have an effect on the cell size and proportions. If the segmentation was made incorrectly, it affected the length and width of the cell. To reduce the amount of error, average of ~20 cells were used, but depending how clumped the cells were the segmentation accuracy varied between cells. Like cell counts, the length to width ratios cannot be used as absolute values and should be used as relative estimates between sample types. No statistical analysis was made due to the uncertainty of the results.

5.3 Challenges

The textiles and coatings reacted differently to the analysis methods. As mentioned previously, the cell counts could not be determined from dopamine bound gelatin coated textiles. This means that if knowing cell amount is important some other method would be required to determine the cell counts when using dopamine bound gelatin. Dopamine bound gelatin also made the cells stay in smaller areas in clumps. This was due to the higher hydrophobicity as the cell suspension stayed as a droplet when plated on dopamine bound gelatin coated materials. This can be both useful and detrimental depending on

usage. If the cells are wanted on specific area of the surface this property could be helpful. If the purpose is to have evenly spread non-clumped cells, it is problematic.

The plain woven derivate PET prevented the detection of cells from anywhere but the top most layer, which could cause problems. However, it had the highest number of cells with clear sarcomere structures and the maturation markers used in this experiment had best values on it. With Geltrex coating it had the highest amounts of cells found. The reason for the good results is unknown. It could be that the autofluorescence from the textile creates a contrast that make the sarcomere structures show more clearly. The results should be tested by using the weave pattern on other textile materials to see if it is what causes the improvements.

5.4 Relevance of the results

In this study the maturity of the hiPSC-CMs was measured only through structural maturation. The used markers were cell shape, sarcomere orientation and sarcomere length. There are other morphological markers that could be tested like T-tubules and cell-to-cell alignment (Tzatzalos et al. 2016). So even in structural maturation there are several parameters that should be studied before the increase in structural maturation can be fully determined. To truly be able to say that the maturation of hiPSC-CM has increased, it has to be also detected in both molecular and functional assays. There are several functional properties that should be tested including calcium transients, electromechanical coupling, contraction and electrophysiology (Tzatzalos et al. 2016).

This study did not test maturation through functional or molecular assays, which means that those have to be tested in the future. The choice was made to keep the size of the study manageable. This study was meant to be basis on which later studies in functionality could be built on. The gene expression was supposed to be tested through qPCR, but unfortunately there were problems with RNA extraction and it was decided to be left out. The possibility to do calcium imaging for these kinds of samples was tested and it was successful. However, we did not test any specific calcium reactions, so no differences between samples were determined.

Overall, more studies should be conducted to determine the optimal textile surface growth platform. The results of this study give an indication on which materials and patterns the future tests could be based on, thus reducing the number of different samples.

6. CONCLUSIONS

The aims of this study were to find a suitable coating to improve the attachment of hiPSC-CMs to textile structure, to find out how those coating materials affect the maturation of hiPSC-CMs and to see if the textiles or the coatings have detrimental effects on analysis methods

This study shows that textiles can be used as growth surfaces for growing hiPSC-CMs and that the textiles increase the structural maturation of the hiPSC-CMs compared to cells grown on flat surface. It also shows that large amounts of cells can be grown on the textiles. However, the efficiency is not great as a large number of cells pass through the textile no matter which coating material is used. None of the coating materials seemed to increase the number of attached cells significantly.

The different coatings provided only small changes in maturation and the textile itself had higher effect. Whether the difference comes from textile material or weave pattern is uncertain and different combinations should be tested. In the present study, the plain woven derivate PET had the best results, but it had the limitation of high autofluorescence that prevented the imaging of other than the top most layer. The same weave pattern should be tested with other material like the PLDLA or standard PET used in this study to see if the results can be obtained on more transparent surfaces.

REFERENCES

Abrams, G.A., Goodman, S.L., Nealey, P.F., Franco, M. and Murphy, C.J. (2000), "Nanoscale topography of the basement membrane underlying the corneal epithelium of the rhesus macaque", *Cell and Tissue Research (2000), Vol. 299 Issue 1, p39-46*.

Acimovic, I., Vilotic, A., Pesl, M., Lacampagne, A., Dvorak, P., Rotrekl, V. & Meli, A.C. (2014). Human Pluripotent Stem Cell-Derived Cardiomyocytes as Research and Therapeu-tic Tools, BioMed Research International, Vol. 2014(512831), pp. 1-14.

Aumailley, M., Bruckner-Tuderman, L., Carter, W.G., Deutzmann, R., Edgar, D., Ekblom, P., Engel, J., Engvall, E., Hohenester, E., Jones, J.C.R., Kleinman, H.K., Marinkovich, M.P., Martin, G.R., Mayer, U., Meneguzzi, G., Miner, J.H., Miyazaki, K., Patarroyo, M., Paulsson, M., Quaranta, V., Sanes, J.R., Sasaki, T., Sekiguchi, K., Sorokin, L.M., Talts, J.F., Tryggvason, K., Uitto, J., Virtanen, I., von der Mark, K., Wewer, U.M., Yamada, Y. and Yurchenco, P.D. (2005), "A simplified laminin nomenclature", *Matrix Biology*, Vol. 24, No. 5, pp. 326-332.

Barnett, V.A. (2005), "Cardiac Myocytes", in P.A. Iaizzo(Ed.), *Handbook of Cardiac Anatomy, Physiology, and Devices* Humana Press, Totowa, NJ, pp. 113-121.

Beck, K., Hunter, I. and Engel, J. (1990), "Structure and function of laminin: anatomy of a multidomain glycoprotein.", *The FASEB Journal*, Vol. 4, No. 2, pp. 148-160.

Benton, G., Arnaoutova, I., George, J., Kleinman, H.K. and Koblinski, J. (2014), "Matrigel: From discovery and ECM mimicry to assays and models for cancer research", *Advanced Drug Delivery Reviews*, Vol. 79–80, pp. 3-18.

Beqqali, A. (2006), "Genome_wide transcriptional profiling of human embryonic stem cells differentiating to cardiomyocytes", *Journal of Molecular & Cellular Cardiology*, Vol. 40, No. 6, pp. 990-991.

Bers, D.M. (2013), "Cardiac Excitation–Contraction Coupling", *Encyclopedia of Biological Chemistry, pp.379-383*, pp. 379-383.

Brandl, F., Sommer, F. and Goepferich, A. (2007), "Rational design of hydrogels for tissue engineering: Impact of physical factors on cell behavior", *Biomaterials*, Vol. 28, No. 2, pp. 134-146.

Burridge, P.W., Anderson, D., Priddle, H., Barbadillo Muñoz, M.D., Chamberlain, S., Allegrucci, C., Young, L.E. and Denning, C. (2007), "Improved Human Embryonic Stem Cell Embryoid Body Homogeneity and Cardiomyocyte Differentiation from a Novel V-96 Plate Aggregation System Highlights Interline Variability", *Stem cells*, Vol. 25, No. 4, pp. 929-938.

Geltrex® LDEV-Free Reduced Growth Factor Basement Membrane Matrix. (2014) Available at: (accessed 12.2.2017) https://tools.thermofisher.com/content/sfs/manuals/Geltrex_LDEVfree_PI.pdf

Burridge, P.W., Keller, G., Gold, J.D. and Wu, J.C. (2012), "Production of De Novo Cardiomyocytes: Human Pluripotent Stem Cell Differentiation and Direct Reprogramming", *Cell Stem Cell,* Vol. 10, No. 1, pp. 16-28.

Giol, E.D., Schaubroeck, D., Kersemans, K., De Vos, F., Van Vlierberghe, S. and Dubruel, P. (2015), "Bio-inspired surface modification of PET for cardiovascular applications: Case study of gelatin", *Colloids and Surfaces B: Biointerfaces,* Vol. 134, pp. 113-121.

Graichen, R., Xu, X., Braam, S.R., Balakrishnan, T., Norfiza, S., Sieh, S., Soo, S.Y., Tham, S.C., Mummery, C., Colman, A., Zweigerdt, R. and Davidson, B.P. (2008), "Enhanced cardiomyogenesis of human embryonic stem cells by a small molecular inhibitor of p38 MAPK", *Differentiation,* Vol. 76, No. 4, pp. 357-370. Available at: http://www.sciencedirect.com/science/article/pii/S0301468109600803.

Han, J., Wu, Q., Xia, Y., Wagner, M.B. and Xu, C. (2016), "Cell alignment induced by anisotropic electrospun fibrous scaffolds alone has limited effect on cardiomyocyte maturation", *Stem Cell Research,* Vol. 16, No. 3, pp. 740-750.

He, J. (2003), "Human embryonic stem cells develop into multiple types of cardiac myocytes - Action potential characterization", *Circulation research,* Vol. 93, No. 1, pp. 32-39.

Hynes, R.O. and Yamada, K.M. (1982), "Fibronectins: Multifunctional Modular Glycoproteins", *The Journal of cell biology,* Vol. 95, No. 2, pp. 369-377.

Janik, K., Popeda, M., Peciak, J., Rosiak, K., Smolarz, M., Treda, C., Rieske, P., Stoczynska-Fidelus, E. and Ksiazkiewicz, M. (2016), "Efficient and simple approach to inÂ vitro culture of primary epithelial cancer cells", *Bioscience reports,* Vol. 36, No. 6, pp. e00423.

Javed, F., Al Amri, M.D., Kellesarian, S.V., Al-Askar, M., Al-Kheraif, A.A. and Romanos, G.E. (2016), "Laminin coatings on implant surfaces promote osseointegration: Fact or fiction?", *Archives of Oral Biology,* Vol. 68, pp. 153-161.

Jukes, J., Both, S., Post, J., Blitterswijk, C.v., Karperien, M. and Boer, J.d. (2008), "Chapter 1 - Stem cells", in C.v. Blitterswijk, , P. Thomsen, et al(Eds.), *Tissue Engineering* Academic Press, Burlington, pp. 1-26.

Junnila A. (2016) Human Induced Pluripotent Stem Cell Derived Cardiomyocytes Grown on Woven Polyethylene Terephthalate Textile. Available at: (accessed 16.11.2016) http://dspace.cc.tut.fi/dpub/bitstream/handle/123456789/24024/junnila.pdf?sequence=1&isAllowed=y

Juthani, N., Howell, C., Ledoux, H., Sotiri, I., Kelso, S., Kovalenko, Y., Tajik, A., Vu, T.L., Lin, J.J., Sutton, A. and Aizenberg, J. (2016), "Infused polymers for cell sheet release", *Scientific Reports,* Vol. 6, pp. 26109.

Kadler, K.E., Baldock, C., Bella, J. and Boot-Handford, R. (2007), "Collagens at a glance", *Journal of cell science,* Vol. 120, No. 12, pp. 1955.

Kartasalo, K., Pölönen, R., Ojala, M., Rasku, J., Lekkala, J., Aalto-Setälä, K. and Kallio, P. (2015), "CytoSpectre: a tool for spectral analysis of oriented structures on cellular and subcellular levels", *BMC Bioinformatics,* Vol. 16, No. 1, pp. 1-23.

Kasemo, B. (2002), "Biological surface science", *Surface Science,* Vol. 500, No. 1–3, pp. 656-677.

Kehat, I. (2001), "Human embryonic stem cells can differentiate into myocytes with structural and functional properties of cardiomyocytes", *Journal Of Clinical Investigation,* Vol. 108, No. 3, pp. 407-414.

Khan, J.M., Lyon, A.R. and Harding, S.E. (2013), "The case for induced pluripotent stem cell-derived cardiomyocytes in pharmacological screening", *British journal of pharmacology,* Vol. 169, No. 2, pp. 304-317.

Khan, M., Xu, Y., Hua, S., Johnson, J., Belevych, A., Janssen, P.M.L., Gyorke, S., Guan, J. and Angelos, M.G. (2015), "Evaluation of Changes in Morphology and Function of Human Induced Pluripotent Stem Cell Derived Cardiomyocytes (HiPSC-CMs) Cultured on an Aligned-Nanofiber Cardiac Patch", *PLoS ONE,* Vol. 10, No. 5, pp. e0126338.

Kleinman, H.K. and Martin, G.R. (2005), "Matrigel: Basement membrane matrix with biological activity", *Seminars in cancer biology,* Vol. 15, No. 5, pp. 378-386.

Kleinman, H.K., Philp, D. and Hoffman, M.P. (2003), "Role of the extracellular matrix in morphogenesis", *Current opinion in biotechnology,* Vol. 14, No. 5, pp. 526-532.

Kujala, V. (2012), "Human pluripotent stem cell derived cardiomyocytes: differentiation, analysis and disease modeling", No. Tampere University Press, pp. 44-45.

Kurosawa, H. (2007), "Methods for inducing embryoid body formation: in vitro differentiation system of embryonic stem cells", *Journal of Bioscience and Bioengineering,* Vol. 103, No. 5, pp. 389-398.

Laske, T.G. and Iaizzo, P.A. (2005), "The Cardiac Conduction System", in P.A. Iaizzo(Ed.), *Handbook of Cardiac Anatomy, Physiology, and Devices* Humana Press, Totowa, NJ, pp. 123-136.

Lockhart, M., Wirrig, E., Phelps, A. and Wessels, A. (2011), "Extracellular Matrix and Heart Development", *Birth defects research.Part A, Clinical and molecular teratology*, Vol. 91, No. 6, pp. 535-550.

Luckenbill-Edds, L. (1997), "Laminin and the mechanism of neuronal outgrowth", *Brain Research Reviews*, Vol. 23, No. 1–2, pp. 1-27.

Luna, J.I., Ciriza, J., Garcia-Ojeda, M.E., Kong, M., Herren, A., Lieu, D.K., Li, R.A., Fowlkes, C.C., Khine, M. and McCloskey, K.E. (2011), "Multiscale Biomimetic Topography for the Alignment of Neonatal and Embryonic Stem Cell-Derived Heart Cells", *Tissue Engineering Part C: Methods*, Vol. 17, No. 5, pp. 579-588.

Ma, Z., Mao, Z. and Gao, C. (2007), "Surface modification and property analysis of biomedical polymers used for tissue engineering", *Colloids and Surfaces B: Biointerfaces*, Vol. 60, No. 2, pp. 137-157.

Massumi, M., Pourasgari, F., Nalla, A., Batchuluun, B., Nagy, K., Neely, E., Gull, R., Nagy, A. and Wheeler, M.B. (2016), "An Abbreviated Protocol for In Vitro Generation of Functional Human Embryonic Stem Cell-Derived Beta-Like Cells", *PLoS ONE*, Vol. 11, No. 10, pp. e0164457.

McDonald, J.H. 2014. Handbook of Biological Statistics, 3rd ed. Sparky House Publishing, Baltimore, Maryland.

Muiznieks, L.D. and Keeley, F.W. (2013), "Molecular assembly and mechanical properties of the extracellular matrix: A fibrous protein perspective", *Biochimica et Biophysica Acta (BBA) - Molecular Basis of Disease*, Vol. 1832, No. 7, pp. 866-875.

Mummery, C., Ward-van Oostwaard, D., Doevendans, P., Spijker, R., van, d.B., Hassink, R., van, d.H., Opthof, T., Pera, M., de, l.R., Passier, R. and Tertoolen, L. (2003), "Differentiation of Human Embryonic Stem Cells to Cardiomyocytes", *Circulation*, Vol. 107, No. 21, pp. 2733.

Ng, E.S., Davis, R.P., Azzola, L., Stanley, E.G. and Elefanty, A.G. (2005), "Forced aggregation of defined numbers of human embryonic stem cells into embryoid bodies fosters robust, reproducible hematopoietic differentiation", *Blood*, Vol. 106, No. 5, pp. 1601.

Nunes, S.S., Miklas, J.W., Liu, J., Aschar-Sobbi, R., Xiao, Y., Zhang, B., Jiang, J., Masse, S., Gagliardi, M., Hsieh, A., Thavandiran, N., Laflamme, M.A., Nanthakumar, K., Gross,

G.J., Backx, P.H., Keller, G. and Radisic, M. (2013), "Biowire: a platform for maturation of human pluripotent stem cell-derived cardiomyocytes", *Nat Meth,* Vol. 10, No. 8, pp. 781-787.

Oberwallner, B., Brodarac, A., Anić, P., Šarić, T., Wassilew, K., Neef, K., Choi, Y. and Stamm, C. (2014), "Human cardiac extracellular matrix supports myocardial lineage commitment of pluripotent stem cells†", *European Journal of Cardio-Thoracic Surgery,* Vol. 47, No. 3, pp. 416-425.

Ohta, R., Niwa, A., Taniguchi, Y., Suzuki, N.M., Toga, J., Yagi, E., Saiki, N., Nishinaka-Arai, Y., Okada, C., Watanabe, A., Nakahata, T., Sekiguchi, K. and Saito, M.K. (2016), "Laminin-guided highly efficient endothelial commitment from human pluripotent stem cells", *Scientific Reports,* Vol. 6, pp. 35680.

Passier, R., Oostwaard, D.W., Snapper, J., Kloots, J., Hassink, R.J., Kuijk, E., Roelen, B., de la Riviere, A.B. and Mummery, C. (2005), "Increased Cardiomyocyte Differentiation from Human Embryonic Stem Cells in Serum-Free Cultures", *Stem cells,* Vol. 23, No. 6, pp. 772-780.

Patterson, J., Martino, M.M. and Hubbell, J.A. (2010), "Biomimetic materials in tissue engineering", *Materials Today,* Vol. 13, No. 1–2, pp. 14-22.

Penton, C.M., Badarinarayana, V., Prisco, J., Powers, E., Pincus, M., Allen, R.E. and August, P.R. (2016), "Laminin 521 maintains differentiation potential of mouse and human satellite cell-derived myoblasts during long-term culture expansion", *Skeletal Muscle,* Vol. 6, pp. 44.

Potts, J.R. and Campbell, I.D. (1996), *Structure and function of fibronectin modules*.

Radisic, M., Park, H., Shing, H., Consi, T., Schoen, F.J., Langer, R., Freed, L.E. and Vunjak-Novakovic, G. (2004), "Functional assembly of engineered myocardium by electrical stimulation of cardiac myocytes cultured on scaffolds", *Proceedings of the National Academy of Sciences,* Vol. 101, No. 52, pp. 18129-18134.

Rao, C., Prodromakis, T., Kolker, L., Chaudhry, U.A.R., Trantidou, T., Sridhar, A., Weekes, C., Camelliti, P., Harding, S.E., Darzi, A., Yacoub, M.H., Athanasiou, T. and Terracciano, C.M. (2013), "The effect of microgrooved culture substrates on calcium cycling of cardiac myocytes derived from human induced pluripotent stem cells", *Biomaterials,* Vol. 34, No. 10, pp. 2399-2411.

Ravenscroft, S.M., Pointon, A., Williams, A.W., Cross, M.J. and Sidaway, J.E. (2016), "Cardiac Non-myocyte Cells Show Enhanced Pharmacological Function Suggestive of Contractile Maturity in Stem Cell Derived Cardiomyocyte Microtissues", *Toxicological Sciences,* Vol. 152, No. 1, pp. 99-112.

Rodina, A.V., Tenchurin, T.K., Saprykin, V.P., Shepelev, A.D., Mamagulashvili, V.G., Grigorâ€™ev, T.E., Lukanina, K.I., Orekhov, A.S., Moskaleva, E.Y. and Chvalun, S.N. (2016), "Migration and Proliferative Activity of Mesenchymal Stem Cells in 3D Polylactide Scaffolds Depends on Cell Seeding Technique and Collagen Modification", *Bulletin of experimental biology and medicine,* Vol. 162, No. 1, pp. 120-126.

Salick, M.R., Napiwocki, B.N., Sha, J., Knight, G.T., Chindhy, S.A., Kamp, T.J., Ashton, R.S. and Crone, W.C. (2014), "Micropattern width dependent sarcomere development in human ESC-derived cardiomyocytes", *Biomaterials,* Vol. 35, No. 15, pp. 4454-4464.

Shandilya, U.K., Sharma, A., Sodhi, M., Kapila, N., Kishore, A., Mohanty, A., Kataria, R., Malakar, D. and Mukesh, M. (2016), "Matrixâ€ based threeâ€ dimensional culture of buffalo mammary epithelial cells showed higher induction of genes related to milk protein and fatty acid metabolism", *Cell biology international,* Vol. 40, No. 2, pp. 232-238.

Shin, H., Jo, S. and Mikos, A.G. (2003), "Biomimetic materials for tissue engineering", *Biomaterials,* Vol. 24, No. 24, pp. 4353-4364.

Snir, M. (2003), "Assessment of the ultrastructural and proliferative properties of human embryonic stem cell-derived cardiomyocytes", *American Journal Of Physiology-Heart And Circulatory Physiology,* Vol. 285, No. 6, pp. H2355-Heart.

Soofi, S.S., Last, J.A., Liliensiek, S.J., Nealey, P.F. and Murphy, C.J. (2009), "The elastic modulus of Matrigel™ as determined by atomic force microscopy", *Journal of structural biology,* Vol. 167, No. 3, pp. 216-219.

Stevens, M.M. and George, J.H. (2005), "Exploring and Engineering the Cell Surface Interface", *Science,* Vol. 310, No. 5751, pp. 1135-1138. Available at: http://science.sciencemag.org/content/310/5751/1135.abstract.

Takahashi, K., Tanabe, K., Ohnuki, M., Narita, M., Ichisaka, T., Tomoda, K. and Yamanaka, S. (2007), "Induction of Pluripotent Stem Cells from Adult Human Fibroblasts by Defined Factors", *Cell,* Vol. 131, No. 5, pp. 861-872.

Takahashi, K. and Yamanaka, S. (2006), "Induction of Pluripotent Stem Cells from Mouse Embryonic and Adult Fibroblast Cultures by Defined Factors", *Cell,* Vol. 126, No. 4, pp. 663-676.

Timpl, R., Rohde, H., Robey, P.G., Rennard, S.I., Foidart, J.M. and Martin, G.R. (1979), "Laminin--a glycoprotein from basement membranes.", *Journal of Biological Chemistry,* Vol. 254, No. 19, pp. 9933-9937.

Tulloch, N.L., Muskheli, V., Razumova, M.V., Korte, F.S., Regnier, M., Hauch, K.D., Pabon, L., Reinecke, H. and Murry, C.E. (2011), "Growth of Engineered Human Myocardium With Mechanical Loading and Vascular Coculture", *Circulation research*, Vol. 109, No. 1, pp. 47-59.

Tzatzalos, E., Abilez, O.J., Shukla, P. and Wu, J.C. (2016), "Engineered heart tissues and induced pluripotent stem cells: Macro- and microstructures for disease modeling, drug screening, and translational studies", *Advanced Drug Delivery Reviews*, Vol. 96, pp. 234-244.

Ventre, M., Causa, F. and Netti, P.A. (2012), "Determinants of cell material crosstalk at the interface: towards engineering of cell instructive materials", *Journal of the Royal Society Interface*, Vol. 9, No. 74, pp. 2017-2032.

Wang, Y., Yang, H. and Regenstein, J.M. (2008), "Characterization of Fish Gelatin at Nanoscale Using Atomic Force Microscopy", *Food Biophysics*, Vol. 3, No. 2, pp. 269-272.

Weinhaus, A.J. and Roberts, K.P. (2005), "Anatomy of the Human Heart", in P.A. Iaizzo(Ed.), *Handbook of Cardiac Anatomy, Physiology, and Devices* Humana Press, Totowa, NJ, pp. 51-79.

Wilson, K., Stuart, S.J., Garcia, A. and Latour, R.A. (2004), "A molecular modeling study of the effect of surface chemistry on the adsorption of a fibronectin fragment spanning the 7–10th type III repeats", *Journal of Biomedical Materials Research Part A*, Vol. 69A, No. 4, pp. 686-698.

Wolbert, L., Jessell, T., Lawrence, P., Meyerowitz, E., Robertson, E. and Smith, J. (2007), *Principles of development*, 3rd ed.

World Health Organization (2015). Cardiovascular diseases (CVDs), Available (accessed on 26.5.2016): http://www.who.int/mediacentre/factsheets/fs317/en/

Xu, C., Inokuma, M.S., Denham, J., Golds, K., Kundu, P., Gold, J.D. and Carpenter, M.K. (2001), "Feeder-free growth of undifferentiated human embryonic stem cells", *Nature biotechnology*, Vol. 19, No. 10, pp. 971.

Xu, X.Q., Graichen, R., Soo, S.Y., Balakrishnan, T., Bte Rahmat, S.N., Sieh, S., Tham, S.C., Freund, C., Moore, J., Mummery, C., Colman, A., Zweigerdt, R. and Davidson, B.P. (2008), "Chemically defined medium supporting cardiomyocyte differentiation of human embryonic stem cells", *Differentiation*, Vol. 76, No. 9, pp. 958-970. Available at: http://www.sciencedirect.com/science/article/pii/S0301468109600335.

Yang, H., Wang, Y., Regenstein, J.M. and Rouse, D.B. (2007), "Nanostructural Characterization of Catfish Skin Gelatin Using Atomic Force Microscopy", *Journal of Food Science,* Vol. 72, No. 8, pp. C430-C440.

Yang, L., Soonpaa, M.H., Adler, E.D., Roepke, T.K., Kattman, S.J., Kennedy, M., Henckaerts, E., Bonham, K., Abbott, G.W., Linden, R.M., Field, L.J. and Keller, G.M. (2008), "Human cardiovascular progenitor cells develop from a KDR+ embryonic-stem-cell-derived population", *Nature,* Vol. 453, No. 7194, pp. 524-528.

Yang, X., Pabon, L. and Murry, C.E. (2014), "Engineering Adolescence: Maturation of Human Pluripotent Stem Cell–Derived Cardiomyocytes", *Circulation research,* Vol. 114, No. 3, pp. 511-523.

Zhang, J., Klos, M., Wilson, G.F., Herman, A.M., Lian, X., Raval, K.K., Barron, M.R., Hou, L., Soerens, A.G., Yu, J., Palecek, S.P., Lyons, G.E., Thomson, J.A., Herron, T.J., Jalife, J. and Kamp, T.J. (2012), "Extracellular Matrix Promotes Highly Efficient Cardiac Differentiation of Human Pluripotent Stem Cells: The Matrix Sandwich Method", *Circulation research,* Vol. 111, No. 9, pp. 1125-1136.